

# Achieving Material Robustness via Symmetric Stress Finite Element Discretizations <sup>\*</sup>

Pablo Brubeck<sup>a</sup>, Charles Parker<sup>b</sup>, Umberto Zerbinati<sup>a</sup>

<sup>a</sup>*University of Oxford, Mathematics Institute, Woodstock Road, Oxford, OX2 6GG, Oxfordshire, United Kingdom*

<sup>b</sup>*U.S. Naval Research Laboratory, 4555 Overlook Ave. S.W., Washington, 20375, DC, USA*

---

## Abstract

When discretizing symmetric stress tensors in variational problems arising in continuum mechanics, one has to choose how to enforce the symmetry of the stress tensor: (i) strongly by requiring the discrete tensors to be pointwise symmetric or (ii) weakly by introducing a Lagrange multiplier. For  $H(\text{div})$ -conforming finite element discretizations of Hellinger–Reissner elasticity and velocity–stress formulations of incompressible flow, where symmetry of the Cauchy stress tensor is tied to the conservation of angular momentum, we show that this choice may substantially impact the accuracy of the numerical scheme. Through a series of benchmark problems featuring anisotropic constitutive laws inspired by fiber reinforced material, liquid crystal polymer networks, and polar fluids, we show that schemes enforcing symmetry weakly can yield arbitrarily poor stress approximations – even for zero-stress configurations. However, schemes enforcing symmetry strongly deliver accurate stress approximations independently of the constitutive law, a property we term *material robustness*. We present a unifying theory that rigorously explains this behavior.

*Keywords:* finite element, elasticity, incompressible flow, stress elements

*2020 MSC:* 65N30, 74S05, 76M10

---

## 1. Introduction

Variational formulations appearing in many applications involve spaces of symmetric tensors. Perhaps the most well-known is the Hellinger-Reissner formulation of elasticity<sup>1</sup> [2, 3, 4], where the Cauchy and second Piola-Kirchhoff stress tensors are symmetric, corre-

---

<sup>\*</sup>This project has received funding through the UKRI Digital Research Infrastructure Programme through the Science and Technology Facilities Council’s Computational Science Centre for Research Communities (CoSeC). CP was supported by an appointment to the NRC Research Associateship Program at the U.S. Naval Research Laboratory, administered by the Fellowships Office of the National Academies of Sciences, Engineering, and Medicine. UZ gratefully acknowledges the Erwin Schrödinger International Institute for Mathematics and Physics (ESI) for supporting the stay in Vienna where this paper was completed. Distribution Statement A. Approved for public release: distribution is unlimited.

<sup>1</sup>See [1] for an English translation of Hellinger’s work [2]

sponding to the preservation of angular momentum <sup>2</sup>. Other examples include the linearized strain field and the (right) Cauchy-Green tensors in intrinsic formulations of elasticity [5], the bending-moments tensor in a mixed formulation of Reissner-Mindlin plates [6], the elasticity tensor in linear Cosserat elasticity [7, 8], and the viscous stress tensor in incompressible flow [9] and in multicomponent convection-diffusion [10], to name a few.

When designing discretizations for these problems, one must decide whether to enforce symmetry of the tensor strongly (pointwise) or weakly (e.g. with a Lagrange multiplier). For  $H(\text{div})$ -conforming finite element discretizations of symmetric tensors, schemes with weak symmetry are often preferred over those with strong symmetry in the literature, largely owing to the perceived complexity of symmetric  $H(\text{div})$ -conforming tensor elements. Indeed, many strongly symmetric tensor elements possess supersmoothness at mesh vertices and/or edges [11, 12, 13, 14, 15] or are macroelements [16, 17, 18, 19, 20] or both [21]. In contrast, schemes with weak symmetry [22, 23, 24, 25, 26, 27, 28, 29] involve more familiar finite element spaces that are readily available in software packages. Generally, weak enforcement of symmetry is not equivalent to strong enforcement unless the finite element spaces are carefully chosen [28], but quasioptimal error estimates for the Hellinger-Reissner problem are available for most of the above schemes; see also [30, 31] for a unified analysis of schemes with strong [30] and weak symmetry [31].

We revisit the importance of strongly versus weakly enforcing the symmetry of the (Cauchy) stress tensor in the context of Hellinger-Reissner formulations of linear elasticity and stress-velocity formulations of incompressible flow. In these contexts, symmetry of the stress tensor is intimately related to the preservation of angular momentum. Preserving physical constraints in discretizations can be crucial in applications. For example, in incompressible flow, discretizations that are pointwise divergence-free lead to so-called *pressure-robust* error estimates, while schemes that are only weakly divergence-free can produce arbitrarily poor velocity approximations to problems with a smooth flow (including no flow) — see [32] for a review and section C for an example. However, the importance of the symmetry constraint in our setting appears to be unaddressed in the literature.

We develop benchmark problems with materials with a variety of constitutive laws, including anisotropic settings inspired by liquid crystal polymer networks and polar fluids, that demonstrate that schemes with weakly imposed symmetry can produce arbitrarily poor stress approximations, even for zero stress configurations. However, most schemes with strongly imposed symmetry do not suffer from this phenomenon, regardless of the constitutive law, a property we call *material robustness*. Fortunately, symmetric tensor elements and other “exotic” finite elements have become increasingly available in open source software packages such as NGSolve [33, 34, 6] and Firedrake [35, 36, 37], which both implement the 2D Hu-Zhang element [14], while the 2D Arnold-Winther element [13] and the 2D and 3D

---

<sup>2</sup>Conservation of angular momentum is not a direct consequence of the symmetry of the Cauchy stress tensor alone as we will see in greater detail later. Yet, for the specific constitutive relations of the Hellinger-Reissner formulation, the symmetry of the Cauchy stress tensor indeed corresponds to the conservation of angular momentum.

Johnson-Mercier-Křížek element [19, 38, 20] are also available in Firedrake (see [36] for a list of other available exotic elements). We additionally develop an abstract theory to unify the construction and behavior of these examples. These insights advocate for the broader adoption of material robust methods in computational continuum mechanics, especially in applications sensitive to rotational invariants.

The remainder of the paper is organized as follows. In section 2, we introduce a general setup for Hellinger-Reissner problems that we consider. We then present a series of numerical examples in section 3 to demonstrate the discrepancies of enforcing symmetry strongly versus weakly that motivate our notion of material robustness. Abstract analysis for general saddle point problems is developed in section 4 to explain the behavior observed in the numerical examples. Finally, we present in section 5 a transient example to show how the observations in section 3 for static problems carry over to the time-dependent setting.

## 2. General problem setup

Consider the balance law for a generic continuum in Eulerian coordinates [39, Result 5.5, Result 7, & Exercise 5.7] in an open domain  $\Omega \subset \mathbb{R}^3$ :

$$\partial_t \rho + \nabla \cdot (\rho \mathbf{u}) = 0, \quad (2.1a)$$

$$\rho (\partial_t \mathbf{u} + \mathbf{u} \cdot \nabla \mathbf{u}) - \nabla \cdot \underline{\underline{\sigma}} = \rho \mathbf{f}, \quad (2.1b)$$

$$\rho (\partial_t \boldsymbol{\eta} + \mathbf{u} \cdot \nabla \boldsymbol{\eta}) - \nabla \cdot \underline{\underline{\zeta}} = \boldsymbol{\xi} + \rho \boldsymbol{\tau}, \quad (2.1c)$$

where  $\rho$  is the density,  $\mathbf{u}$  is the velocity,  $\boldsymbol{\eta}$  is the angular momentum,  $\underline{\underline{\sigma}}$  is the Cauchy stress tensor,  $\underline{\underline{\zeta}}$  is the couple stress tensor<sup>3</sup>,  $\mathbf{f}$  is the body force,  $\boldsymbol{\tau}$  is an external body torque and  $\boldsymbol{\xi}$  is the vectorified form of the antisymmetric part of the stress tensor, i.e.

$$\boldsymbol{\xi} = (\sigma_{32} - \sigma_{23}, \sigma_{13} - \sigma_{31}, \sigma_{21} - \sigma_{12})^\top. \quad (2.2)$$

We remark that (2.1a) expresses the conservation of mass, (2.1b) the conservation of the total linear momentum, and (2.1c) the conservation of the angular momentum. To close the system, the balance laws (2.1) are augmented with initial and boundary conditions and constitutive laws relating the stress tensors  $\underline{\underline{\sigma}}$ ,  $\underline{\underline{\zeta}}$  to the kinematic variables  $\rho$ ,  $\mathbf{u}$ , and  $\boldsymbol{\eta}$ .

It is common to say that the angular momentum is conserved if and only if the antisymmetric part of the Cauchy stress tensor vanishes ( $\boldsymbol{\xi} \equiv \mathbf{0}$ ). In absence of body torques and couple stresses ( $\underline{\underline{\zeta}} \equiv \underline{\underline{0}}$  and  $\boldsymbol{\tau} \equiv \mathbf{0}$ ), this is indeed true, as the angular momentum balance law (2.1c) reduces to

$$\rho (\partial_t \boldsymbol{\eta} + \mathbf{u} \cdot \nabla \boldsymbol{\eta}) = \boldsymbol{\xi}, \quad (2.3)$$

and so angular momentum is conserved (i.e. the material time derivative of  $\boldsymbol{\eta}$  vanishes) if and only if  $\boldsymbol{\xi} \equiv \mathbf{0}$  (i.e.  $\underline{\underline{\sigma}} = \underline{\underline{\sigma}}^\top$ ) — see [39, Exercise 5.7]. In the presence of couple stresses ( $\underline{\underline{\zeta}} \neq \underline{\underline{0}}$ )

---

<sup>3</sup>The couple stress tensor is the analog of the Cauchy stress tensor but with respect to body torque rather than force [39], in the same way that the angular momentum and the body torque are analogous to the velocity and the body force respectively.

and/or external body torques ( $\boldsymbol{\tau} \neq \mathbf{0}$ ), the Cauchy stress tensor may be symmetric even though angular momentum is not conserved, or the angular momentum may be conserved even though the Cauchy stress tensor is not symmetric. We proceed below in a stationary linearized setting where body torques and couple stresses are absent, so the symmetry of the Cauchy stress tensor does indeed correspond to the conservation of angular momentum.

### 2.1. PDE formulation of the linearized static problem

Let  $\Omega \subset \mathbb{R}^d$ ,  $d \in \{2, 3\}$ , be a Lipschitz polyhedral domain. In the three examples below, we assume that the system is in equilibrium and neglect the body torques and couple stresses. For flow problems, we linearize about an equilibrium velocity  $\mathbf{u}_0$  with  $|\mathbf{u}_0| \ll 1$  in  $\Omega$ , and assume that  $\rho \equiv 1$ . In this case, the conservation of mass (2.1a) and linear momentum (2.1b) read

$$\nabla \cdot \mathbf{u} = -\nabla \cdot \mathbf{u}_0 =: g_{\text{div}} \quad \text{and} \quad \nabla \cdot \underline{\underline{\boldsymbol{\sigma}}} = \mathbf{f}, \quad (2.4)$$

where we abuse notation and use  $\mathbf{u}$  to also denote the perturbation velocity. To close (2.1), we require a constitutive law relating the Cauchy stress  $\underline{\underline{\boldsymbol{\sigma}}}$  to the symmetric part of the gradient of the velocity  $\underline{\underline{\boldsymbol{\varepsilon}}}(\mathbf{u}) := (\nabla \mathbf{u} + (\nabla \mathbf{u})^\top)/2$ . Linearizing a generic constitutive law of the form

$$\underline{\underline{\boldsymbol{\sigma}}} = \underline{\underline{G}}(\underline{\underline{\boldsymbol{\varepsilon}}}(\mathbf{u}), q, \underline{\underline{\tilde{H}}}),$$

where  $q$  is the spherical response and  $\underline{\underline{\tilde{H}}}$  is a symmetric tensor associated with some external field, possibly depending nonlinearly on  $\mathbf{u}$  and  $q$ , often leads to a relation of the form

$$\underline{\underline{\boldsymbol{\sigma}}} = 2\mu \underline{\underline{\boldsymbol{\varepsilon}}}(\mathbf{u}) - p \underline{\underline{I}} + \underline{\underline{\tilde{F}}}, \quad (2.5)$$

where  $\mu > 0$  is a parameter (often the viscosity),  $p$  is a Lagrange multiplier enforcing the divergence constraint in (2.4), and  $\underline{\underline{\tilde{F}}}$  is a linearization of  $\underline{\underline{\tilde{H}}}$ . The physical interpretation of  $\underline{\underline{\tilde{F}}}$  varies depending on the continuum we are modelling and will be discussed for each example in section Section 3.

Due to the presence of the term  $\underline{\underline{\tilde{F}}}$  and the nonvanishing bulk viscosity,  $p$  is neither the mechanical nor the thermodynamic pressure [40]. For this reason, it appears compelling from an engineering point of view to eliminate such Lagrange multiplier from our formulation. We take the trace of (2.5) to obtain

$$p = \frac{1}{d} \text{tr} \left( 2\mu \underline{\underline{\boldsymbol{\varepsilon}}}(\mathbf{u}) + \underline{\underline{\tilde{F}}} - \underline{\underline{\boldsymbol{\sigma}}} \right). \quad (2.6)$$

Substituting this relation back into (2.5) gives

$$\underline{\underline{\boldsymbol{\sigma}}}^D = 2\mu \underline{\underline{\boldsymbol{\varepsilon}}}(\mathbf{u})^D + \underline{\underline{\tilde{F}}}^D \implies \underline{\underline{\boldsymbol{\varepsilon}}}(\mathbf{u})^D = \frac{1}{2\mu} \left( \underline{\underline{\boldsymbol{\sigma}}}^D - \underline{\underline{\tilde{F}}}^D \right),$$

where  $\underline{\underline{\sigma}}^D := \underline{\underline{\sigma}} - d^{-1} \text{tr}(\underline{\underline{\sigma}})\mathbb{I}$  is the deviatoric part of  $\underline{\underline{\sigma}}$ . On noting that  $\text{tr} \underline{\underline{\varepsilon}}(\mathbf{u}) = \nabla \cdot \mathbf{u} = g_{\text{div}}$ , we have

$$\underline{\underline{\varepsilon}}(\mathbf{u}) = \frac{1}{2\mu} \underline{\underline{\sigma}}^D - \left( \frac{1}{2\mu} \tilde{\underline{\underline{F}}}^D - \frac{1}{d} g_{\text{div}} \mathbb{I} \right) =: \frac{1}{2\mu} \underline{\underline{\sigma}}^D - \underline{\underline{F}}. \quad (2.7)$$

We also consider solid materials linearized about a zero displacement state. Similar manipulations [39, Chapter 7.1] give rise to constitutive relations of the form

$$\underline{\underline{\varepsilon}}(\mathbf{u}) = \frac{1}{2\mu} \underline{\underline{\sigma}}^D + \frac{1}{d(2\mu + \lambda)} (\text{tr} \underline{\underline{\sigma}})\mathbb{I} - \underline{\underline{F}}, \quad (2.8)$$

where  $\mathbf{u}$  is now the displacement and  $\mu, \lambda > 0$  are material parameters. Since (2.7) is precisely of the form (2.8) with  $\lambda = \infty$ , (2.1) augmented with the constitutive law (2.8) becomes the following for both fluids and solids:

$$\frac{1}{2\mu} \underline{\underline{\sigma}}^D + \frac{1}{d(2\mu + d\lambda)} (\text{tr} \underline{\underline{\sigma}})\mathbb{I} - \underline{\underline{\varepsilon}}(\mathbf{u}) = \underline{\underline{F}} \quad \text{in } \Omega, \quad (2.9a)$$

$$\nabla \cdot \underline{\underline{\sigma}} = \mathbf{f} \quad \text{in } \Omega, \quad (2.9b)$$

$$\mathbf{u} = \mathbf{g} \quad \text{on } \partial\Omega, \quad (2.9c)$$

where  $\mathbf{f}$  encodes the external forces and  $\mathbf{g}$  is the prescribed value of  $\mathbf{u}$  on  $\partial\Omega$ . For simplicity, we assume that  $\underline{\underline{F}}$  is independent of  $\mathbf{u}$  so that (2.9) is a linear system of partial differential equations. If  $\lambda = \infty$ , we additionally require the compatibility condition  $\int_{\partial\Omega} \mathbf{g} \cdot \mathbf{n} \, ds = - \int_{\Omega} \text{tr} \underline{\underline{F}} \, dx$ , which can be seen by taking the trace of (2.9a), integrating over  $\Omega$ , and applying the divergence theorem. The formulation (2.9) for incompressible flow ( $\lambda = \infty$ ) is sometimes called the stress-velocity formulation and, at least in the numerical analysis community, seems to date back to [41] for the design of least-squares finite element methods.

**Remark 2.1.** *Constitutive laws for linear isotropic material with an external anisotropy may also be expressed as*

$$\underline{\underline{\sigma}} = 2\mu \underline{\underline{\varepsilon}}(\mathbf{u}) + \lambda \text{tr}(\underline{\underline{\varepsilon}}(\mathbf{u}))\mathbb{I} + \tilde{\underline{\underline{F}}}. \quad (2.10)$$

Taking the trace of (2.10) gives

$$\text{tr} \underline{\underline{\sigma}} = (2\mu + d\lambda) \text{tr} \underline{\underline{\varepsilon}}(\mathbf{u}) + \text{tr} \tilde{\underline{\underline{F}}} \implies \underline{\underline{\varepsilon}}(\mathbf{u}) = \frac{1}{2\mu} (\underline{\underline{\sigma}} - \tilde{\underline{\underline{F}}}) - \frac{\lambda}{2\mu(2\mu + d\lambda)} \text{tr}(\underline{\underline{\sigma}} - \tilde{\underline{\underline{F}}})\mathbb{I}.$$

After a little more algebraic manipulation, we arrive at (2.8) with

$$\underline{\underline{F}} = \frac{1}{2\mu} \tilde{\underline{\underline{F}}}^D + \frac{1}{d(2\mu + d\lambda)} \text{tr}(\tilde{\underline{\underline{F}}})\mathbb{I}. \quad (2.11)$$

## 2.2. Variational formulation with strong symmetry

We consider a variational formulation of (2.9), also known as the Hellinger-Reissner formulation [2, 3, 4], where  $\mathbf{u}$  and  $\underline{\sigma}$  are independent variables. We use standard notation for Sobolev spaces of scalar-valued functions. For vector- or matrix-valued spaces, we include the codomain in the space; e.g.,  $L^2(\Omega; \mathbb{R}^d)$  is the space of square-integrable vector-valued functions. Other codomains include  $\mathbb{R}_{\text{sym}}^{d \times d}$  the set of symmetric matrices, and  $\mathbb{R}_{\text{skw}}^{d \times d}$  the set of skew-symmetric matrices. We also define matrix-valued spaces with square-integrable divergence

$$\begin{aligned} H(\text{div}; \Omega, \circ) &:= \{ \underline{\tau} \in L^2(\Omega, \circ) : \nabla \cdot \underline{\tau} \in L^2(\Omega, \mathbb{R}^d) \}, & \circ \in \{ \mathbb{R}^{d \times d}, \mathbb{R}_{\text{sym}}^{d \times d} \}, \\ H_*(\text{div}; \Omega, \circ) &:= \left\{ \underline{\tau} \in H(\text{div}; \Omega, \circ) : \int_{\Omega} \text{tr } \underline{\tau} \, dx = 0 \right\}, & \circ \in \{ \mathbb{R}^{d \times d}, \mathbb{R}_{\text{sym}}^{d \times d} \}, \end{aligned}$$

where the divergence of matrix is taken row-wise.

The Hellinger-Reissner formulation of (2.9) then reads as follows: Find  $\underline{\sigma} \in \Sigma^{\text{sym}}$  and  $\mathbf{u} \in V$  such that

$$a(\underline{\sigma}, \underline{\tau}) + b(\underline{\tau}, \mathbf{u}) = \langle \underline{\tau} \mathbf{n}, \mathbf{g} \rangle_{\partial\Omega} + (\underline{F}, \underline{\tau})_{L^2(\Omega)} \quad \forall \underline{\tau} \in \Sigma^{\text{sym}}, \quad (2.12a)$$

$$b(\underline{\sigma}, \mathbf{v}) = (\mathbf{f}, \mathbf{v})_{L^2(\Omega)} \quad \forall \mathbf{v} \in V, \quad (2.12b)$$

where the spaces are chosen as

$$\Sigma^{\text{sym}} := \begin{cases} H(\text{div}; \Omega, \mathbb{R}_{\text{sym}}^{d \times d}) & \text{if } \lambda < \infty, \\ H_*(\text{div}; \Omega, \mathbb{R}_{\text{sym}}^{d \times d}) & \text{if } \lambda = \infty, \end{cases} \quad \text{and} \quad V := L^2(\Omega; \mathbb{R}^d), \quad (2.13)$$

and the bilinear forms are given by

$$a(\underline{\sigma}, \underline{\tau}) := \frac{1}{2\mu} (\underline{\sigma}^D, \underline{\tau}^D)_{L^2(\Omega)} + \frac{1}{d(2\mu + d\lambda)} (\text{tr } \underline{\sigma}, \text{tr } \underline{\tau})_{L^2(\Omega)}, \quad (2.14a)$$

$$b(\underline{\sigma}, \mathbf{v}) := (\nabla \cdot \underline{\sigma}, \mathbf{v})_{L^2(\Omega)}. \quad (2.14b)$$

The angle brackets  $\langle \cdot, \cdot \rangle_{\partial\Omega}$  in (2.12a) denote the duality pairing between  $H^{-1/2}(\partial\Omega; \mathbb{R}^d)$  and  $H^{1/2}(\partial\Omega; \mathbb{R}^d)$ . Since the normal trace  $\underline{\tau} \mapsto \tau \mathbf{n}|_{\partial\Omega}$  is a bounded operator from  $H(\text{div}; \Omega, \mathbb{R}^{d \times d})$  to  $H^{-1/2}(\partial\Omega; \mathbb{R}^d)$ , all terms in (2.12) are well-defined provided that  $\mathbf{f} \in L^2(\Omega; \mathbb{R}^d)$  and  $\mathbf{g} \in H^{1/2}(\partial\Omega; \mathbb{R}^d)$ , which we shall assume for the remainder of the manuscript. We review the well-posedness of (2.12) in section A and note here that (2.12) admits a unique solution.

A standard conforming Galerkin approximation of (2.12) reads as follows: Find  $\underline{\sigma}_h \in \Sigma_h^{\text{sym}}$  and  $\mathbf{u}_h \in V_h$  such that

$$a(\underline{\sigma}_h, \underline{\tau}_h) + b(\underline{\tau}_h, \mathbf{u}_h) = \langle \underline{\tau}_h \mathbf{n}, \mathbf{g} \rangle_{\partial\Omega} + (\underline{F}, \underline{\tau}_h)_{L^2(\Omega)} \quad \forall \underline{\tau}_h \in \Sigma_h^{\text{sym}}, \quad (2.15a)$$

$$b(\underline{\sigma}_h, \mathbf{v}_h) = (\mathbf{f}, \mathbf{v}_h)_{L^2(\Omega)} \quad \forall \mathbf{v}_h \in V_h, \quad (2.15b)$$

where  $\Sigma_h^{\text{sym}} \subset \Sigma^{\text{sym}}$  and  $V_h \subset V$  are finite dimensional spaces. As mentioned in section 1, conforming finite elements for  $\Sigma^{\text{sym}}$  have been recently adopted in open source software. One

challenge is constructing a finite element space  $\Sigma_h^{\text{sym}}$  that is both  $H(\text{div}; \Omega, \mathbb{R}^{d \times d})$ -conforming and symmetric. Another challenge is choosing a space  $V_h$  such that both the discrete kernel coercivity condition

$$a(\underline{\sigma}_h, \underline{\sigma}_h) \geq \alpha_h^{\text{sym}} \|\underline{\sigma}_h\|_{\text{div}}^2 \quad \forall \underline{\sigma}_h \in \{\underline{\tau}_h \in \Sigma_h^{\text{sym}} : b(\underline{\tau}_h, \mathbf{v}_h) = 0 \ \forall \mathbf{v}_h \in V_h\} \quad (2.16)$$

holds for some  $\alpha_h^{\text{sym}} > 0$  and the discrete inf-sup condition holds

$$\beta_h^{\text{sym}} := \inf_{\mathbf{v}_h \in V_h} \sup_{\underline{\tau}_h \in \Sigma_h^{\text{sym}}} \frac{b(\underline{\tau}_h, \mathbf{v}_h)}{\|\underline{\tau}_h\|_{\text{div}} \|\mathbf{v}_h\|} > 0. \quad (2.17)$$

Here, we use  $\|\cdot\|_{\text{div}}$  to denote the  $H(\text{div})$  norm and  $\|\cdot\|$  to denote the  $L^2$  norm. Nevertheless, more elements satisfying these conditions are appearing in the literature; we refer to the recent manuscripts [16, 18] and references therein for a review. The same arguments in the beginning of this section show that any scheme of the form of (2.15) will conserve the angular momentum since  $\underline{\sigma}_h \in \Sigma_h^{\text{sym}}$  is pointwise symmetric.

In the numerical examples below, we consider the following two schemes on a shape regular, conforming simplicial mesh  $\mathcal{T}_h$ :

1. the Johnson-Mercier-Křížek (JMK) scheme (see [19, 20] for  $d = 2$  and [38] for  $d = 3$ ), which takes  $\Sigma_h^{\text{sym}}$  to be  $H(\text{div}; \Omega, \mathbb{R}_{\text{sym}}^{d \times d})$ -conforming piecewise linear matrices on a barycentric refinement of  $\mathcal{T}_h$  and  $V_h$  to be the space of piecewise constants on the barycentrically-refined mesh. See also [18] for an extension to any dimension and for reduced elements.
2. The Hu-Zhang ( $\text{HZ}_k$ ) scheme (see [14] for  $d = 2$  and [15] for  $d = 3$ ). For  $d = 2$ ,  $\Sigma_h^{\text{sym}}$  is the space of  $H(\text{div}; \Omega, \mathbb{R}_{\text{sym}}^{d \times d})$ -conforming piecewise polynomial matrices of degree  $k \geq 3$  that are also continuous at element vertices and  $V_h = \mathcal{P}_{k-1}(\mathcal{T}_h; \mathbb{R}^2)$ , where  $\mathcal{P}_{k-1}(\mathcal{T}_h; \circ)$  is the space of discontinuous piecewise polynomials of degree  $k - 1$  on  $\mathcal{T}_h$  over the space  $\circ$ .

The finite element spaces in the JMK scheme ( $d = 2, 3$ ) and the  $\text{HZ}_k$  schemes ( $d = 2$ ) are implemented in the finite element software package Firedrake [36, 37]. We also note that both schemes satisfy  $\text{div } \Sigma_h^{\text{sym}} = V_h$ , a common feature for strongly symmetric schemes.

### 2.3. Variational formulation with weak symmetry

A more common technique in the literature is to enforce the symmetry constraint weakly. More precisely, we remove the symmetry constraint in  $\Sigma^{\text{sym}}$  and instead enforce symmetry with a Lagrange multiplier: Find  $\underline{\sigma} \in \Sigma$ ,  $\mathbf{u} \in V$ , and  $\underline{\omega} \in \Xi$  such that

$$a(\underline{\sigma}, \underline{\tau}) + b(\underline{\tau}, \mathbf{u}) + c(\underline{\tau}, \underline{\omega}) = \langle \underline{\tau} \mathbf{n}, \mathbf{g} \rangle_{\partial\Omega} + (\underline{F}, \underline{\tau})_{L^2(\Omega)} \quad \forall \underline{\tau} \in \Sigma, \quad (2.18a)$$

$$b(\underline{\sigma}, \mathbf{v}) = (\mathbf{f}, \mathbf{v})_{L^2(\Omega)} \quad \forall \mathbf{v} \in V, \quad (2.18b)$$

$$c(\underline{\sigma}, \underline{\xi}) = 0 \quad \forall \underline{\xi} \in \Xi, \quad (2.18c)$$

where  $V$  is defined in (2.13),

$$\Sigma := \begin{cases} H(\operatorname{div}; \Omega, \mathbb{R}^{d \times d}) & \text{if } \lambda < \infty, \\ H_*(\operatorname{div}; \Omega, \mathbb{R}^{d \times d}) & \text{if } \lambda = \infty, \end{cases} \quad \Xi := L^2(\Omega, \mathbb{R}_{\operatorname{skw}}^{d \times d}), \quad \text{and} \quad c(\underline{\tau}, \underline{\xi}) := (\underline{\tau}, \underline{\xi})_{L^2(\Omega)}. \quad (2.19)$$

Problem (2.18) is also well-posed — see section A for a review. A direct calculation shows that (2.12) and (2.18) have the same solution.

**Remark 2.2.** Note that (2.18c) shows that  $\underline{\sigma}$  is pointwise symmetric, and so taking  $\tau \in C_0^\infty(\Omega; \mathbb{R}_{\operatorname{skw}}^{d \times d})$  in (2.18a) gives

$$0 = a(\underline{\sigma}, \underline{\tau}) + b(\underline{\tau}, \mathbf{u}) + c(\underline{\tau}, \underline{\omega}) = (\operatorname{div} \underline{\tau}, \mathbf{u})_{L^2(\Omega)} + (\underline{\tau}, \underline{\omega})_{L^2(\Omega)} = -\langle \operatorname{skw}(\nabla \mathbf{u}), \underline{\tau} \rangle_\Omega + (\underline{\tau}, \underline{\omega})_{L^2(\Omega)},$$

where we used that  $\underline{F}$  is symmetric,  $\langle \cdot, \cdot \rangle_\Omega$  denotes the action of the distribution, and  $\operatorname{skw}$  denotes the skew-symmetric part of a tensor. Thus, the Lagrange multiplier  $\underline{\omega} = \operatorname{skw}(\nabla \mathbf{u})$ , and we will refer to  $\underline{\omega}$  as the rotation tensor, the tensorization of the “vorticity”  $\nabla \times \mathbf{u}$ .

A standard Galerkin formulation of (2.18) reads as follows: Find  $\underline{\sigma}_h \in \Sigma_h$ ,  $\mathbf{u}_h \in V_h$ , and  $\underline{\omega}_h \in \Xi_h$  such that

$$a(\underline{\sigma}_h, \underline{\tau}_h) + b(\underline{\tau}_h, \mathbf{u}_h) + c(\underline{\tau}_h, \underline{\omega}_h) = \langle \underline{\tau}_h \mathbf{n}, \mathbf{g} \rangle_{\partial\Omega} + (\underline{F}, \underline{\tau}_h)_{L^2(\Omega)} \quad \forall \underline{\tau}_h \in \Sigma_h, \quad (2.20a)$$

$$b(\underline{\sigma}_h, \mathbf{v}_h) = (\mathbf{f}, \mathbf{v}_h)_{L^2(\Omega)} \quad \forall \mathbf{v}_h \in V_h, \quad (2.20b)$$

$$c(\underline{\sigma}_h, \underline{\xi}_h) = 0 \quad \forall \underline{\xi}_h \in \Xi_h, \quad (2.20c)$$

where  $\Sigma_h \subset \Sigma$ ,  $V_h \subset V$ , and  $\Xi_h \subset \Xi$  are finite dimensional spaces.  $H(\operatorname{div}; \mathbb{R}^{d \times d})$ -conforming spaces  $\Sigma_h$  can be constructed by taking each row of a matrix in  $\Sigma_h$  to be a (vector-valued)  $H(\operatorname{div}; \Omega, \mathbb{R}^d)$ -conforming element — some examples are below. Note that  $V_h$  and  $\Xi_h$  do not have any continuity requirement, so their construction is also simple. Here, the challenge lies in choosing spaces so that both the discrete kernel coercivity condition

$$a(\underline{\sigma}_h, \underline{\sigma}_h) \geq \alpha_h \|\underline{\sigma}_h\|_{\operatorname{div}}^2 \quad \forall \underline{\sigma}_h \in \{\underline{\tau}_h \in \Sigma_h : b(\underline{\tau}_h, \mathbf{v}_h) + c(\underline{\tau}_h, \underline{\xi}_h) = 0 \quad \forall \mathbf{v}_h \in V_h, \quad \forall \underline{\xi}_h \in \Xi_h\} \quad (2.21)$$

holds for some  $\alpha_h > 0$  and the discrete inf-sup condition holds

$$\beta_h := \inf_{\substack{\mathbf{v}_h \in V_h \\ \underline{\xi}_h \in \Xi_h}} \sup_{\substack{\underline{\tau}_h \in \Sigma_h \\ \underline{\xi}_h \in \Xi_h}} \frac{b(\underline{\tau}_h, \mathbf{v}_h) + c(\underline{\tau}_h, \underline{\xi}_h)}{\|\underline{\tau}_h\|_{\operatorname{div}} (\|\mathbf{v}_h\| + \|\underline{\xi}_h\|)} > 0. \quad (2.22)$$

Typically, one chooses the spaces so that  $\operatorname{div} \Sigma_h = V_h$ , and (2.21) follows from the corresponding result on the continuous level. Thus, inf-sup compatibility (2.22) is the main difficulty. We refer to Chapter 9 of [42] for a review of many available choices. Generally,  $\underline{\sigma}_h \in \Sigma_h$  given by (2.20) will not be pointwise symmetric; thus, the arguments in the beginning of this section show that angular momentum is *not* conserved. However, we do have weak conservation in the sense of (2.20c).

In the examples below, we consider the following two schemes defined on a shape-regular, conforming mesh  $\mathcal{T}_h$ :

1. The PEERS scheme [23] defined for  $d = 2$  as follows. For  $\ell \geq 1$ , let  $\mathcal{RT}_\ell(\mathcal{T}_h)$  be the standard Raviart-Thomas space [43],  $\mathcal{CG}_\ell(\mathcal{T}_h)$  the space of continuous piecewise polynomials of degree  $\ell$ , and  $\mathcal{B}_\ell(\mathcal{T}_h)$  the subspace of  $\mathcal{CG}_\ell(\mathcal{T}_h)$  that vanishes on all mesh edges. Then,  $\Sigma_h$ ,  $V_h$ , and  $\Xi_h$  are chosen as follows:

$$\Sigma_h = (\mathcal{RT}_1(\mathcal{T}_h) \oplus \text{curl } \mathcal{B}_3(\mathcal{T}_h))^2, \quad (2.23a)$$

$$V_h = \mathcal{P}_0(\mathcal{T}_h; \mathbb{R}^2), \quad (2.23b)$$

$$\Xi_h = \left\{ \begin{bmatrix} 0 & \phi \\ -\phi & 0 \end{bmatrix} : \phi \in \mathcal{CG}_1(\mathcal{T}_h) \right\}, \quad (2.23c)$$

where curl is a  $\pi/2$  counterclockwise rotation of the gradient and the notation in (2.23a) means that the rows of matrices in of  $\Sigma_h$  belong to  $\mathcal{RT}_1(\mathcal{T}_h) \oplus \text{curl } \mathcal{B}_3(\mathcal{T}_h)$ . The extension of PEERS to  $d = 3$  can be found in [42, Example 9.4.2] and to higher-order in [42, Example 9.4.1].

2. The Arnold-Falk-Winther (AFW $_k$ ) scheme [24] defined for  $d \in \{2, 3\}$  and  $k \geq 1$  as follows. For  $\ell \geq 1$ , let  $\mathcal{BDM}_\ell(\mathcal{T}_h)$  denote the standard Brezzi-Douglas-Marini [44] space of order  $\ell$ . Then,  $\Sigma_h$ ,  $V_h$ , and  $\Xi_h$  are chosen as follows:

$$\Sigma_h = \mathcal{BDM}_k(\mathcal{T}_h)^d, \quad V_h = \mathcal{P}_{k-1}(\mathcal{T}_h; \mathbb{R}^d), \quad \text{and} \quad \Xi_h = \mathcal{P}_{k-1}(\mathcal{T}_h; \mathbb{R}_{\text{skw}}^{d \times d}). \quad (2.24)$$

At lowest order ( $k = 1$ ), this scheme is similar to the hybridized scheme in [22].

**Remark 2.3.** For all the schemes above, we also incorporate the constraint  $\int_\Omega \text{tr } \underline{\sigma} \, dx = 0$  into the space  $\Sigma_h^{\text{sym}}$  or  $\Sigma_h$  if  $\lambda = \infty$ . However, this is only for theoretical purposes. In the implementation, this additional constraint is instead applied as a post-processing procedure. See section B for additional discussion.

**Remark 2.4.** Suppose we start with a constitutive law of the form (2.10) with  $\lambda < \infty$  and perform the change of variables  $\tilde{\underline{\sigma}} = \underline{\sigma} - \underline{\tilde{F}}$ . Then,  $\tilde{\underline{\sigma}}$  and  $\mathbf{u}$  satisfy the same law (2.9a) with  $\underline{F} \equiv 0$ . Thus, in this setting, one could always assume without loss of generality that  $\underline{F} \equiv 0$ . Similarly, if  $g_{\text{div}} \equiv 0$ , one could also eliminate  $\underline{F}$  when  $\lambda = \infty$ . However, we do not pursue this simplification as we consider  $g_{\text{div}} \neq 0$  and want to highlight the potential behavior in the nonlinear setting where such a change of variable may not be possible.

**Remark 2.5.** That we only consider “enclosed flow” or “pure displacement” boundary conditions ( $\mathbf{u} = \mathbf{g}$  on  $\partial\Omega$ ) is neither essential to the behavior of the methods nor the analysis presented below. If we instead have  $\mathbf{u} = \mathbf{g}_1$  on  $\Gamma_D$  and  $\underline{\sigma}\mathbf{n} = \mathbf{g}_2$  on  $\Gamma_T$  for some partition of the boundary  $\partial\Omega = \Gamma_D \cup \Gamma_T$ , then the condition  $\underline{\sigma}\mathbf{n} = \mathbf{g}_2$  becomes an essential boundary condition on the stress spaces in (2.15) and (2.20). However, the Firedrake library, which we use for the numerical examples below, does not support the strong imposition of essential boundary conditions for finite elements with supersmoothness, which includes the stress space in the Hu-Zhang scheme.

### 3. Examples

We now consider three different anisotropy terms  $\underline{\underline{F}}$  in (2.12a) inspired by the constitutive laws of various materials. In each example, we construct a manufactured solution so that  $\mathbf{f} \equiv \mathbf{0}$ ,  $\underline{\underline{\sigma}} \equiv \underline{\underline{0}}$ , and  $\mathbf{u} \neq \mathbf{0}$  but known analytically. We fix  $\mu = 10^{-4}$  and choose  $\lambda$  depending on the example. However, we note that the behavior of the methods highlighted below is insensitive to the choice of  $\mu$ .

We set  $\Omega = (0, 1)^d$  and generate an unstructured mesh using ngsPETS<sub>c</sub> [45] with `maxh` as specified in each example. These meshes avoid a superconvergence phenomenon we observed for the PEERS scheme on a structured mesh. We then measure the convergence of the JMK and or HZ<sub>3</sub> scheme described at the end of section 2.2 for the strongly symmetric formulation (2.15) and the PEERS (only if  $d = 2$ ) and AFW <sub>$k$</sub>  schemes,  $k \geq 1$ , described at the end of section 2.3, for the weakly symmetric formulation (2.20). We compute the stress errors  $\|\underline{\underline{\sigma}} - \underline{\underline{\sigma}}_h\|_{\text{div}}$  and displacement errors  $\|\mathbf{u} - \mathbf{u}_h\|$  on a sequence of meshes uniformly refined by bisecting every edge. For the weakly symmetric schemes, we also compute the error in the rotation tensor  $\|\underline{\underline{\omega}} - \underline{\underline{\omega}}_h\|$ , where we recall from Remark 2.2 that  $\underline{\underline{\omega}} = \text{skw}(\nabla \mathbf{u})$ .

All the examples are implemented using the Firedrake [37] library. The code to reproduce the results can be found at [46]. A discussion of the linear solvers appears in section B.

#### 3.1. Example 1: Linear isotropic solid in 2D

We first consider the case of a linear isotropic solid with no external anisotropy ( $\underline{\underline{F}} \equiv \underline{\underline{0}}$ ). In this case, the only displacement fields that are stress-free are rigid body motions. Here, we are not interested in the nearly incompressible regime, so we set  $\lambda = 1$  and `maxh` = 1/8. See section A for some remarks on the stability and well-posedness of the Hellinger-Reissner formulation in the limit as  $\lambda \rightarrow \infty$ .

We choose the exact displacement to be the following rigid body motion

$$\mathbf{u}(x, y) = \delta \begin{bmatrix} -y \\ x \end{bmatrix} \implies \underline{\underline{\sigma}} \equiv \underline{\underline{0}}, \quad \mathbf{g} = \mathbf{u}|_{\partial\Omega}, \quad \text{and} \quad \underline{\underline{\omega}} = \delta \begin{bmatrix} 0 & 1 \\ -1 & 0 \end{bmatrix}, \quad (3.1)$$

where  $\delta \in \{10, 10^3, 10^5\}$  is a scaling parameter that we vary. Note that the exact rotation tensor satisfies  $\underline{\underline{\omega}} \in \Xi_h$  for both the PEERS and the AFW <sub>$k$</sub>  schemes for all  $k \geq 1$ .

The numerical results are displayed in Figure 1. Note that all three methods produce about the same errors and the displacement is converging linearly. As we will see in section 4.3,  $\underline{\underline{\sigma}}_h \equiv \underline{\underline{0}}$  in exact arithmetic for each of the schemes. Here, the growth in the error as  $\delta$  increases arises from the accumulation of roundoff errors that are proportional to  $\delta$ . The same phenomenon is observed for discretizations of incompressible flow — see section C.

#### 3.2. Example 2: Transversely isotropic solids in 2D

We now introduce a transverse isotropy by adding a directional contribution aligned with a prescribed vector field, i.e. taking  $\underline{\underline{F}} = \delta(\boldsymbol{\nu} \otimes \boldsymbol{\nu})$  in (2.10), where the director  $\boldsymbol{\nu} : \Omega \rightarrow \mathbb{R}^2$  specifies the axis of transverse isotropy and  $\delta > 0$  is a parameter. Such material laws arise in colloidal suspensions [47] and fiber-reinforced materials [48]. Note that  $\underline{\underline{F}}$  is then given by (2.11).

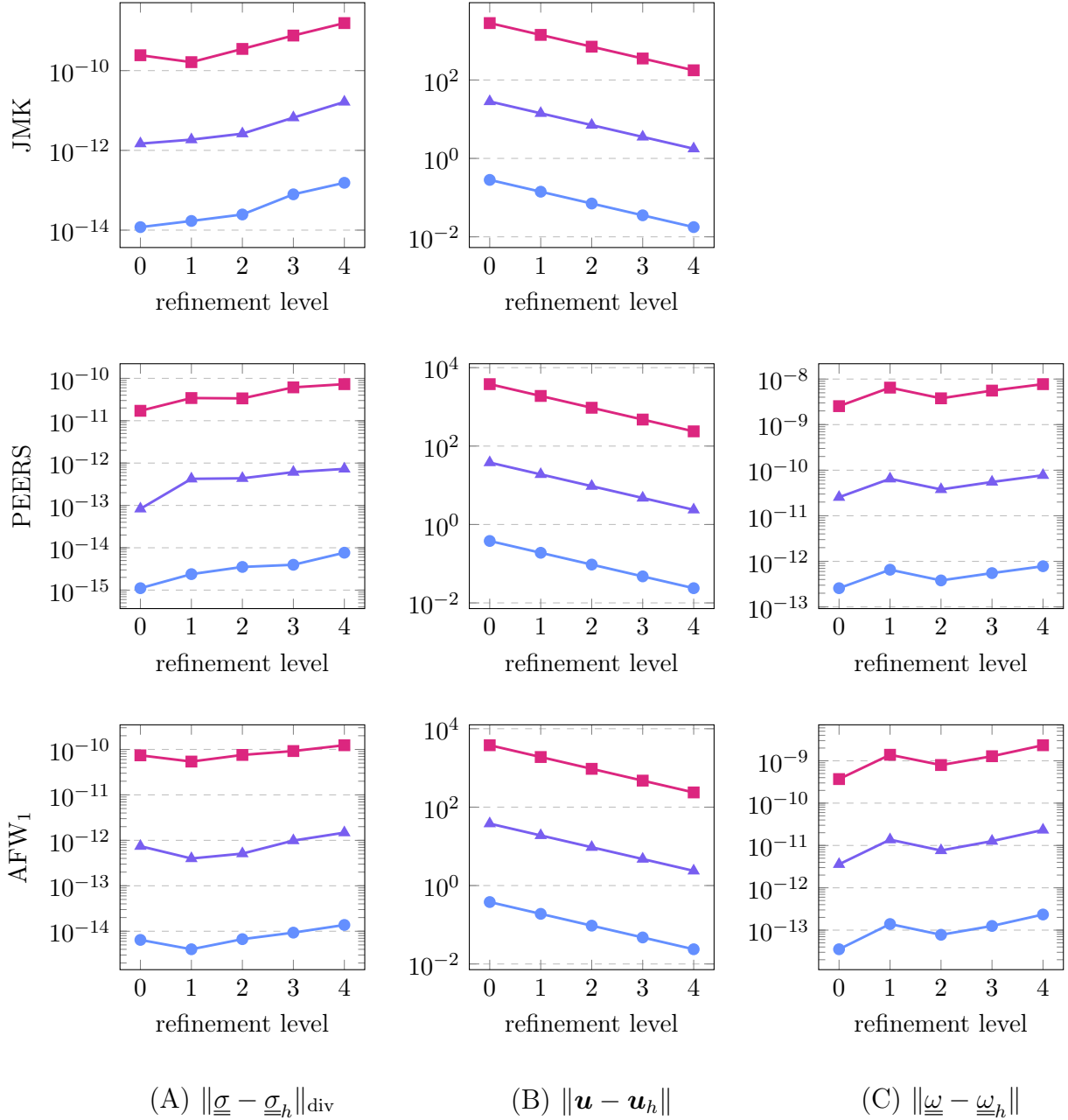


Figure 1: Numerical results for the 2D linear isotropic solid example in section 3.1 for  $\delta = 10$  ( $\bullet$ ),  $\delta = 10^3$  ( $\blacktriangle$ ), and  $\delta = 10^5$  ( $\blacksquare$ ) with the JMK scheme (first row), the PEERS scheme (second row), and AFW<sub>1</sub> scheme (third row). (A) the stress errors in  $H(\text{div}; \Omega, \mathbb{R}_{\text{sym}}^{2 \times 2})$  (B) the displacement errors in  $L^2(\Omega; \mathbb{R}^2)$ , and (C)  $L^2(\Omega; \mathbb{R}_{\text{skw}}^{2 \times 2})$  errors in the Lagrange multiplier  $\underline{\underline{\omega}}$  (only for the weakly symmetric methods). Observe that three methods produce nearly the same errors.

Suppose that we choose exact displacement  $\mathbf{u}$ , the director  $\boldsymbol{\nu}$ , and the boundary data  $\mathbf{g}$  as follows:

$$\mathbf{u} = -\frac{\delta}{2\mu} \left[ x^2y + xy^2 + \frac{1}{3}y^3 + \frac{2}{3}x^3 \right], \quad \boldsymbol{\nu}(x, y) = \begin{bmatrix} x \\ x + y \end{bmatrix}, \quad \text{and} \quad \mathbf{g} = \mathbf{u}|_{\partial\Omega}, \quad (3.2)$$

where  $\delta \in \{10, 10^3, 10^5\}$  is again a scaling parameter that we vary. The rotation tensor is given by

$$\underline{\underline{\omega}} = \frac{\delta(x^2 + xy + y^2)}{2\mu} \begin{bmatrix} 0 & 1 \\ -1 & 0 \end{bmatrix}. \quad (3.3)$$

A direct calculation shows that for any choice of  $\mu$  and  $\delta$ ,  $\underline{\underline{\sigma}} = \lambda(\text{tr} \underline{\underline{\omega}}) \underline{\underline{\mathbb{I}}}$ , and so  $\underline{\underline{\sigma}} \equiv \underline{\underline{0}}$  if and only if  $\lambda = 0$ . Thus, we prescribe  $\lambda = 0$  and again set  $\mathbf{maxh} = 1/8$ .

The numerical results are displayed in Figure 2. First note that the JMK scheme gives results that have the same behavior as the previous example. Again, we will see below in section 4.3 that for the JMK scheme in exact arithmetic,  $\underline{\underline{\sigma}}_h \equiv \underline{\underline{0}}$ . In contrast to the previous example, the PEERS and AFW<sub>1</sub> schemes produce large errors in the stress  $\underline{\underline{\sigma}}$  and the rotation tensor  $\underline{\underline{\omega}}$  that also scale like  $\delta$ . These errors cannot be explained by the accumulation of roundoff errors or stopping criteria of the iterative solver. To investigate this phenomenon further, we also consider the AFW<sub>k</sub> scheme with larger  $k$ . The results for  $k \in \{1, 2, 3\}$  are displayed in Figure 3, which show that at exactly  $k = 3$ , the scheme recovers the behavior in the previous example. Namely, the stress and rotation tensor errors are zero up to roundoff error and solver tolerances. Note that the exact rotation tensor satisfies  $\underline{\underline{\omega}} \in \Xi_h$  for the AFW<sub>k</sub> scheme for all  $k \geq 3$ , while in the previous example we have  $\underline{\underline{\omega}} \in \Xi_h$  for all the schemes. Thus, the inclusion  $\underline{\underline{\omega}} \in \Xi_h$  seems to be crucial for the robustness of stress errors with respect to  $\delta$  for the weakly symmetric schemes. This finding will be confirmed theoretically in section 4.

### 3.3. Example 3: Polar Fluids

In the previous two examples, we have seen that the schemes for the strongly symmetric formulation (2.15) and the weakly symmetric formulation (2.20) behaved similarly with respect to the scaling parameter  $\delta$  provided that the exact rotation tensor satisfied  $\underline{\underline{\omega}} \in \Xi_h$ . In the example in section 3.2, the condition  $\underline{\underline{\omega}} \in \Xi_h$  required sufficiently high-order elements. We now turn to an example where the inclusion  $\underline{\underline{\omega}} \in \Xi_h$  is not possible for any piecewise polynomial space  $\Xi_h$ .

Consider polar fluids — fluids composed by constituents endowed with a molecular orientation that while retaining fluid flow properties exhibit anisotropic elastic response. Following Leslie's and Ericksen's works [47, 49, 50] if we introduce a director field  $\boldsymbol{\nu} : \Omega \rightarrow \mathbb{R}^d$  describing the average orientation of the molecular constituents, we can assume the stress response of the polar fluid subject to the divergence constraint  $\nabla \cdot \mathbf{u} = g_{\text{div}}$  is given by

$$\underline{\underline{\sigma}} = 2\mu \underline{\underline{\varepsilon}}(\mathbf{u}) - p \underline{\underline{I}} + K_F \nabla \boldsymbol{\nu}^\top \nabla \boldsymbol{\nu}, \quad (3.4)$$

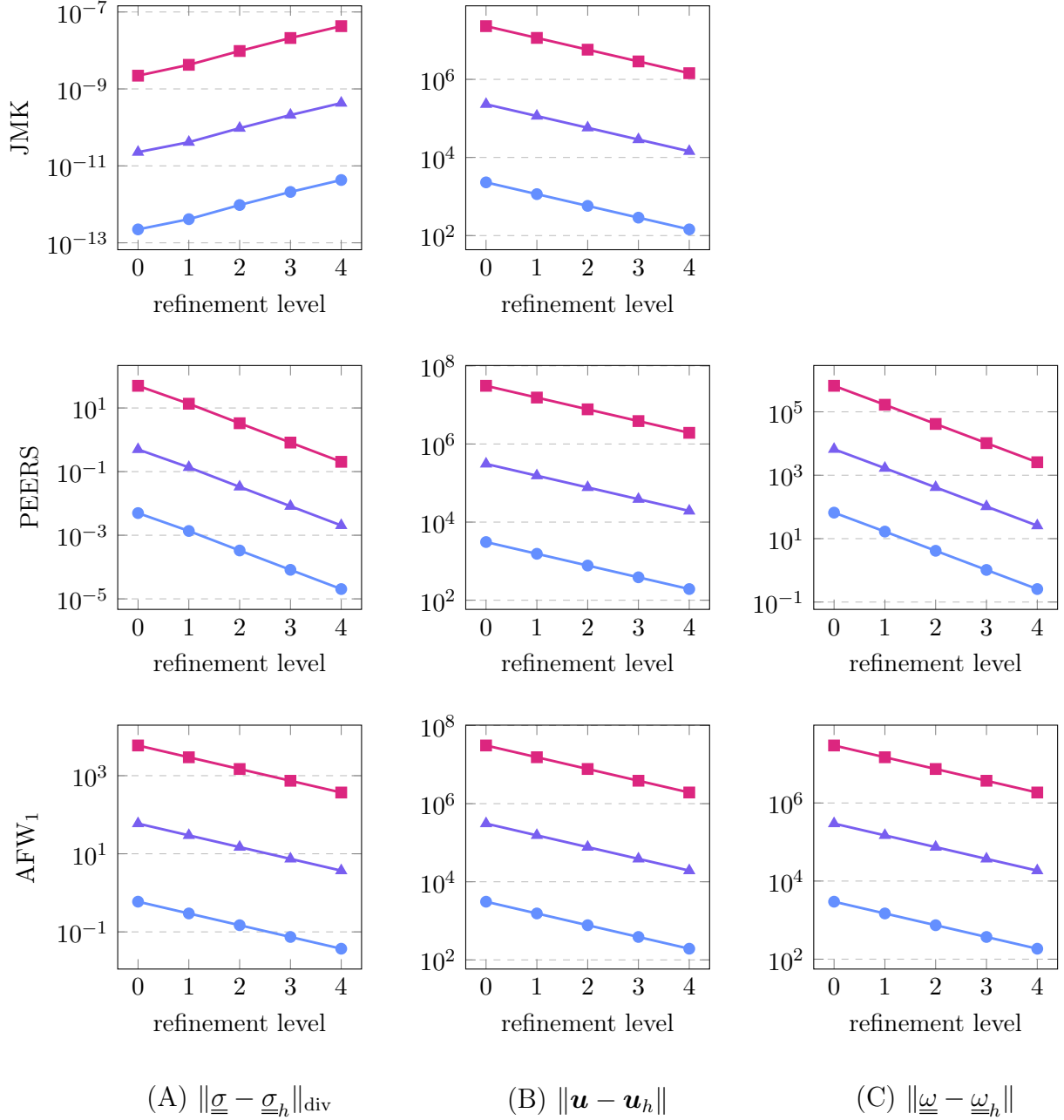


Figure 2: Numerical results for the 2D transversely isotropic example in section 3.2 for  $\delta = 10$  ( $\bullet$ ),  $\delta = 10^3$  ( $\blacktriangle$ ), and  $\delta = 10^5$  ( $\blacksquare$ ) with the JMK, PEERS, and  $\text{AFW}_1$  schemes. The errors are displayed as in Figure 1. Observe that the stress errors for the PEERS and  $\text{AFW}_1$  schemes are no longer zero up to roundoff errors, in contrast to Figure 1, even though both examples satisfy  $\underline{\underline{\sigma}} \equiv \underline{\underline{0}}$ . Here, the exact rotation tensor  $\underline{\underline{\omega}}$  is not included in the discrete space  $\Xi_h$  for the weakly symmetric schemes.

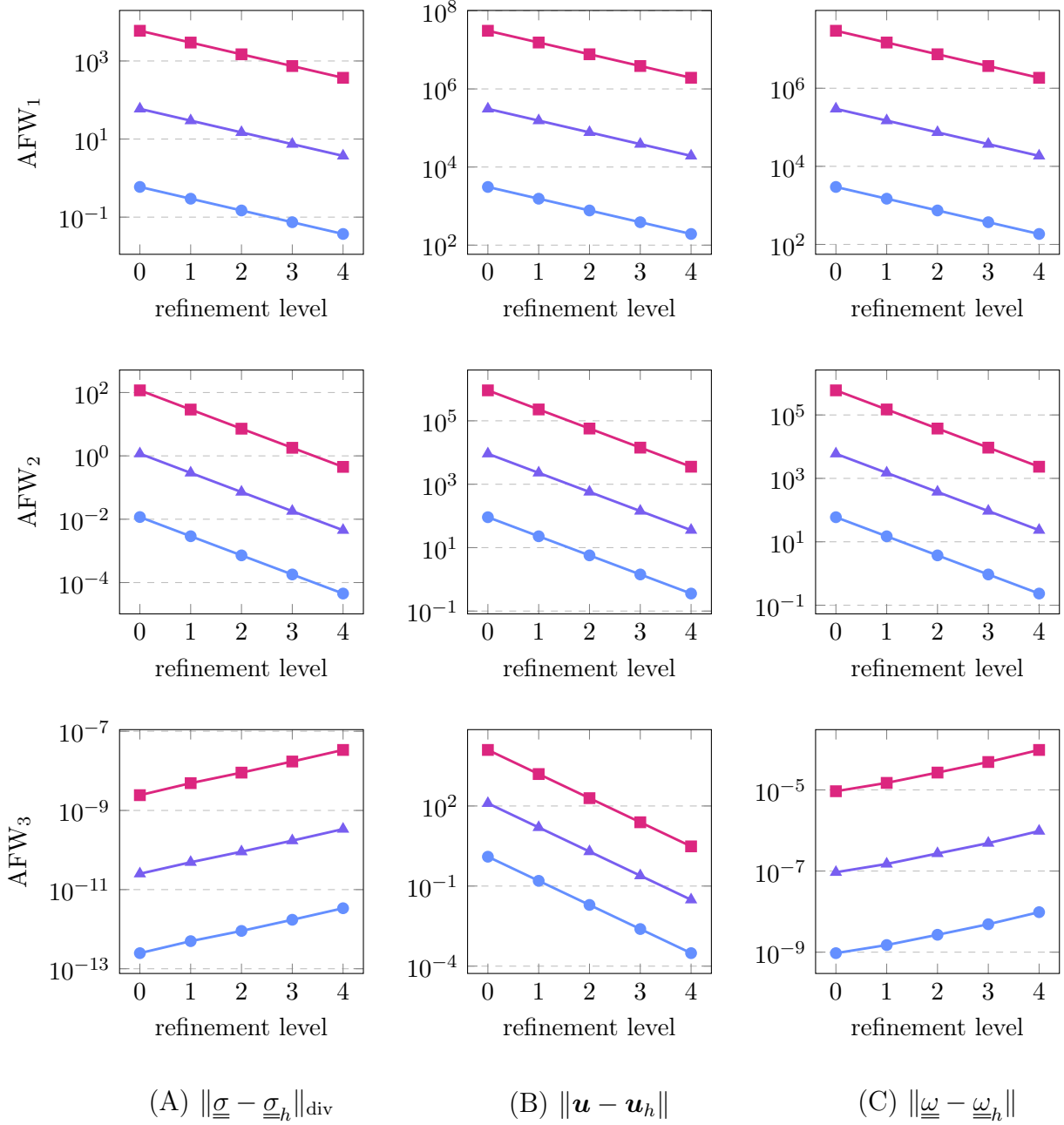


Figure 3: Numerical results for the 2D transversely isotropic example in section 3.2 for  $\delta = 10$  ( $\bullet$ ),  $\delta = 10^3$  ( $\blacktriangle$ ), and  $\delta = 10^5$  ( $\blacksquare$ ) with the  $\text{AFW}_k$ ,  $k \in \{1, 2, 3\}$ , schemes. The errors are displayed as in Figure 1. Observe that the stress errors for the  $\text{AFW}_1$  and  $\text{AFW}_2$  schemes are not zero up to roundoff errors, even though  $\underline{\underline{\sigma}} \equiv \underline{\underline{0}}$ . Meanwhile,  $\text{AFW}_3$  produces a stress-free solution. Note that the exact rotation tensor  $\underline{\underline{\omega}}$  is only included in the discrete space  $\Xi_h$  for the  $\text{AFW}_k$  scheme with  $k \geq 3$ .

where  $\mu$  is the fluid viscosity,  $p : \Omega \rightarrow \mathbb{R}$  is a Lagrange multiplier enforcing the divergence constraint, and  $K_F : \Omega \rightarrow \mathbb{R}$  is known as the Frank constant. In general,  $K_F$  and  $\boldsymbol{\nu}$  depend nonlinearly on  $\mathbf{u}$  and  $p$  (see e.g. [51, eq. (6.17)] for compressible, inviscid liquid crystals). Here, we assume that  $K_F$  and  $\boldsymbol{\nu}$  are given so that (3.4) is of the form (2.5). To complete the specification of the variational form (2.12) or (2.18), we also need to specify  $\int_{\Omega} \text{tr } \underline{\underline{\sigma}} \, dx$ , which we take to be zero since  $\underline{\underline{\sigma}} \equiv \underline{\underline{0}}$  in the examples below.

### 3.3.1. Two dimensions

Suppose we choose the velocity and pressure to be

$$\mathbf{u}(x, y) = -\frac{\delta}{\mu} \begin{bmatrix} -\cos(x) \cosh(y) \\ \sin(x) \sinh(y) \end{bmatrix} \quad \text{and} \quad p(x, y) = -\delta \sin(x) \cosh(y)$$

and  $\boldsymbol{\nu}$  and  $K_F$  to be

$$\boldsymbol{\nu}(x, y) = \begin{bmatrix} x \\ y \end{bmatrix} \quad \text{and} \quad K_F(x, y) = \delta \sin(x) \cosh(y).$$

Then, a direct calculation shows that for any value of  $\mu$  and  $\delta$ , we have

$$\underline{\underline{\sigma}} \equiv \underline{\underline{0}} \quad \text{and} \quad \underline{\underline{\omega}} = -\frac{\delta}{\mu} \begin{bmatrix} 0 & -\cos(x) \sinh(y) \\ \cos(x) \sinh(y) & 0 \end{bmatrix}.$$

Note that the inclusion  $\underline{\underline{\omega}} \in \Xi_h$  is not possible for any piecewise polynomial space  $\Xi_h$ .

The numerical results for the JMK scheme with  $\text{maxh} = 1/32$ , the HZ<sub>3</sub> scheme with  $\text{maxh} = 1/8$ , and the AFW<sub>3</sub> scheme with  $\text{maxh} = 1/8$  are displayed in Figure 4. We observe that for the strongly symmetric schemes, the stress errors behave similarly as in the previous two examples, while for the weakly symmetric scheme AFW<sub>3</sub>, the stress errors are well above solver tolerances and scale like  $\delta$ .

### 3.3.2. Three dimensions

Similar phenomena occur in three dimensions. Consider the following velocity and pressure fields:

$$\mathbf{u}(x, y, z) = -\frac{\delta}{2\mu} \begin{bmatrix} x + 2 \sin(y) \\ \frac{3}{2}y + \frac{1}{4} \sin(2y) \\ z \end{bmatrix} \quad \text{and} \quad p(x, y, z) \equiv 0$$

and  $\boldsymbol{\nu}$  and  $K_F$  to be

$$\boldsymbol{\nu}(x, y, z) = \begin{bmatrix} x + \sin(y) \\ y \\ z \end{bmatrix} \quad \text{and} \quad K_F(x, y, z) = \delta.$$

The numerical results for the JMK and AFW<sub>1</sub> schemes with  $\text{maxh} = 1/4$  are displayed in Figure 5. Note that the behavior of the methods is analogous to the behavior in two dimensions.

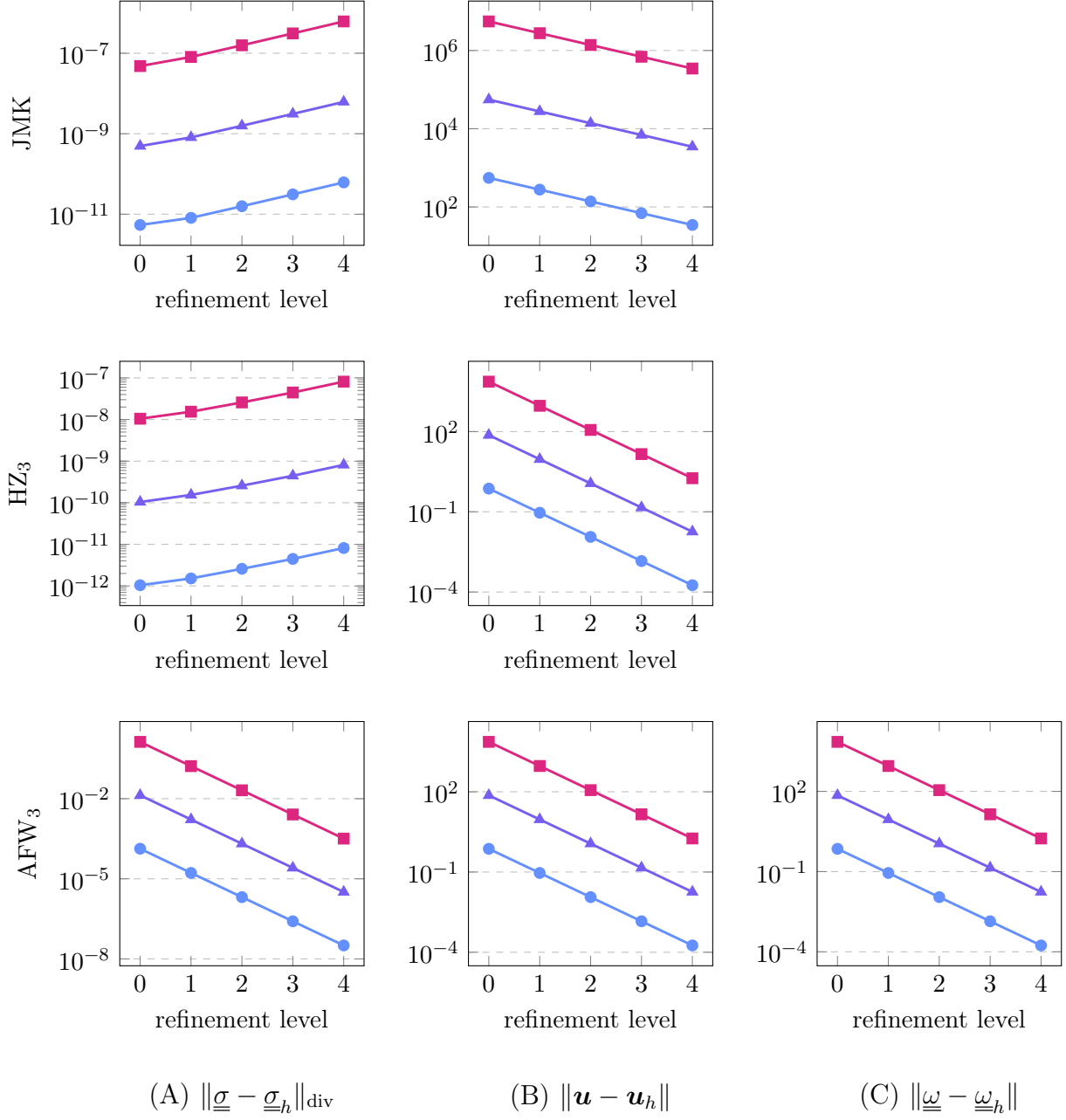


Figure 4: Numerical results for the 2D polar fluid example in section 3.3.1 for  $\delta = 10$  ( $\bullet$ ),  $\delta = 10^3$  ( $\blacktriangle$ ), and  $\delta = 10^5$  ( $\blacksquare$ ) with the JMK scheme, the HZ<sub>3</sub> scheme, and the AFW<sub>3</sub> scheme. The errors are displayed as in Figure 1. Observe that the strongly symmetric schemes JMK and HZ<sub>3</sub> have similar behavior to the strongly symmetric schemes in the previous two examples, while the stress errors for AFW<sub>3</sub> are well above solver tolerances and scale like  $\delta$ .

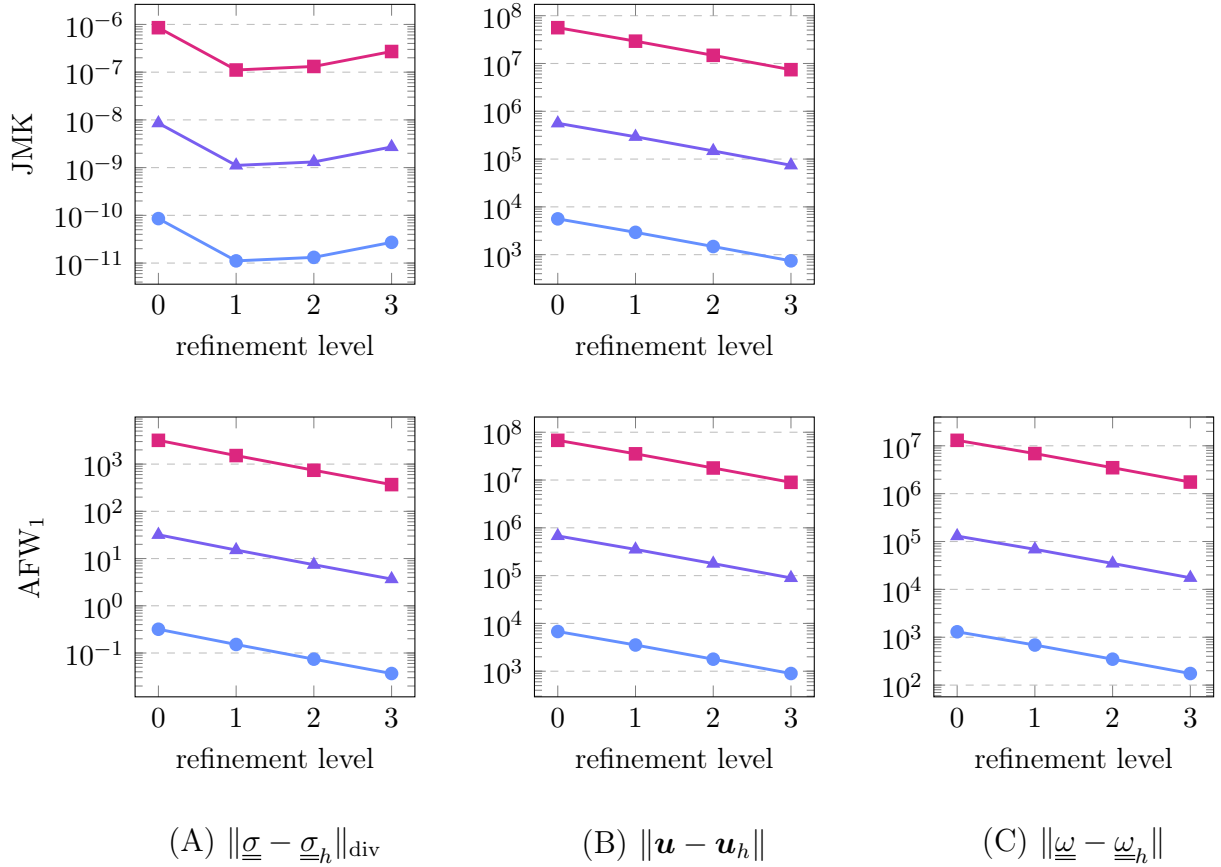


Figure 5: Numerical results for the 3D polar fluid example in section 3.3.2 for  $\delta = 10$  ( $\bullet$ ),  $\delta = 10^3$  ( $\blacktriangle$ ), and  $\delta = 10^5$  ( $\blacksquare$ ) with the JMK and AFW<sub>1</sub> schemes. The errors are displayed as in Figure 1. Observe that the strongly symmetric schemes JMK has similar behavior to the strongly symmetric schemes in the previous two examples, while the stress errors for AFW<sub>1</sub> are well above solver tolerances and scale like  $\delta$ .

### 3.4. Summarizing example and material robustness

We have seen that any scheme that preserves angular momentum, i.e. is strongly symmetric, always produces a zero stress state, up to roundoff errors, whenever the true stress vanishes. However, the schemes that violate the angular momentum conservation, i.e. the weakly symmetric ones, can produce arbitrarily large stress states unless the exact rotation tensor belongs to the discrete space  $\Xi_h$ . In general, the solution to (2.9) will be a linear combination of stress-free and stressed states. To illustrate the behavior of the schemes in this case, we add a smooth component to the exact velocity in the 2D polar fluid example in section 3.3.1:

$$\mathbf{u}(x, y) = -\frac{\delta}{\mu} \begin{bmatrix} -\cos(x) \cosh(y) \\ \sin(x) \sinh(y) \end{bmatrix} + \begin{bmatrix} \cos(x)y \\ \sin(y) \end{bmatrix} \quad \text{and} \quad p(x, y) = -\delta \sin(x) \cosh(y)$$

and define  $\underline{\sigma}$  so that (2.9a) holds with  $\lambda = \infty$  for the same choice of  $\underline{F}$  as in section 3.3.1. In particular, the exact stress is independent of  $\delta$ . In Figure 6, we observe that as  $\delta \rightarrow \infty$  the stress error curves overlap up to solver tolerances for strongly symmetric schemes, while the stress errors scale like  $\delta$  for weakly symmetric schemes.

In summary, the stress errors for approximations to (2.9) may be sensitive to shifts in the exact solution by a stress-free state. The discrete stresses from schemes that exactly preserve angular momentum are unaffected by these shifts, while the stresses from schemes that violate the preservation of angular momentum produce arbitrarily large errors. Based on these observations, we say a scheme is *material robust* for the linearized system (2.9) if the approximation to any stress-free state is stress-free pointwise. As a consequence, the stress errors of a material robust scheme for (2.9) remain bounded whenever the exact solution to (2.9) is shifted by any zero-stress state. Thus, the results in this section suggest that the schemes preserving angular momentum are material robust, while the schemes that do not are not material robust. This finding will be confirmed rigorously in the next section.

## 4. Supporting theory

We now seek a general theory to explain the numerical results above and rigorously justify the material robustness of the strongly symmetric schemes. We first present a series of results in an abstract Hilbert space setting and then apply them to the particular examples above. Let  $\mathcal{V}$  and  $\mathcal{Q}$  be Hilbert spaces with inner products  $(\cdot, \cdot)_{\mathcal{V}}$  and  $(\cdot, \cdot)_{\mathcal{Q}}$  and induced norms  $\|\cdot\|_{\circ} := \sqrt{(\cdot, \cdot)_{\circ}}$  for  $\circ \in \{\mathcal{V}, \mathcal{Q}\}$ . Let  $A(\cdot, \cdot) : \mathcal{V} \times \mathcal{V} \rightarrow \mathbb{R}$  and  $B(\cdot, \cdot) : \mathcal{V} \times \mathcal{Q} \rightarrow \mathbb{R}$  be bounded bilinear forms. For  $F \in \mathcal{V}'$  and  $G \in \mathcal{Q}'$ , consider a generic saddle point problem: Find  $u \in \mathcal{V}$  and  $p \in \mathcal{Q}$  such that

$$A(u, v) + B(v, p) = F(v) \quad \forall v \in \mathcal{V}, \tag{4.1a}$$

$$B(u, q) = G(q) \quad \forall q \in \mathcal{Q}. \tag{4.1b}$$

We assume that the bilinear forms  $A(\cdot, \cdot)$  and  $B(\cdot, \cdot)$  satisfy the usual Babuška-Brezzi conditions (see e.g. [42, Theorem 4.2.3]) so that solutions to (4.1) exist, are unique, and depend

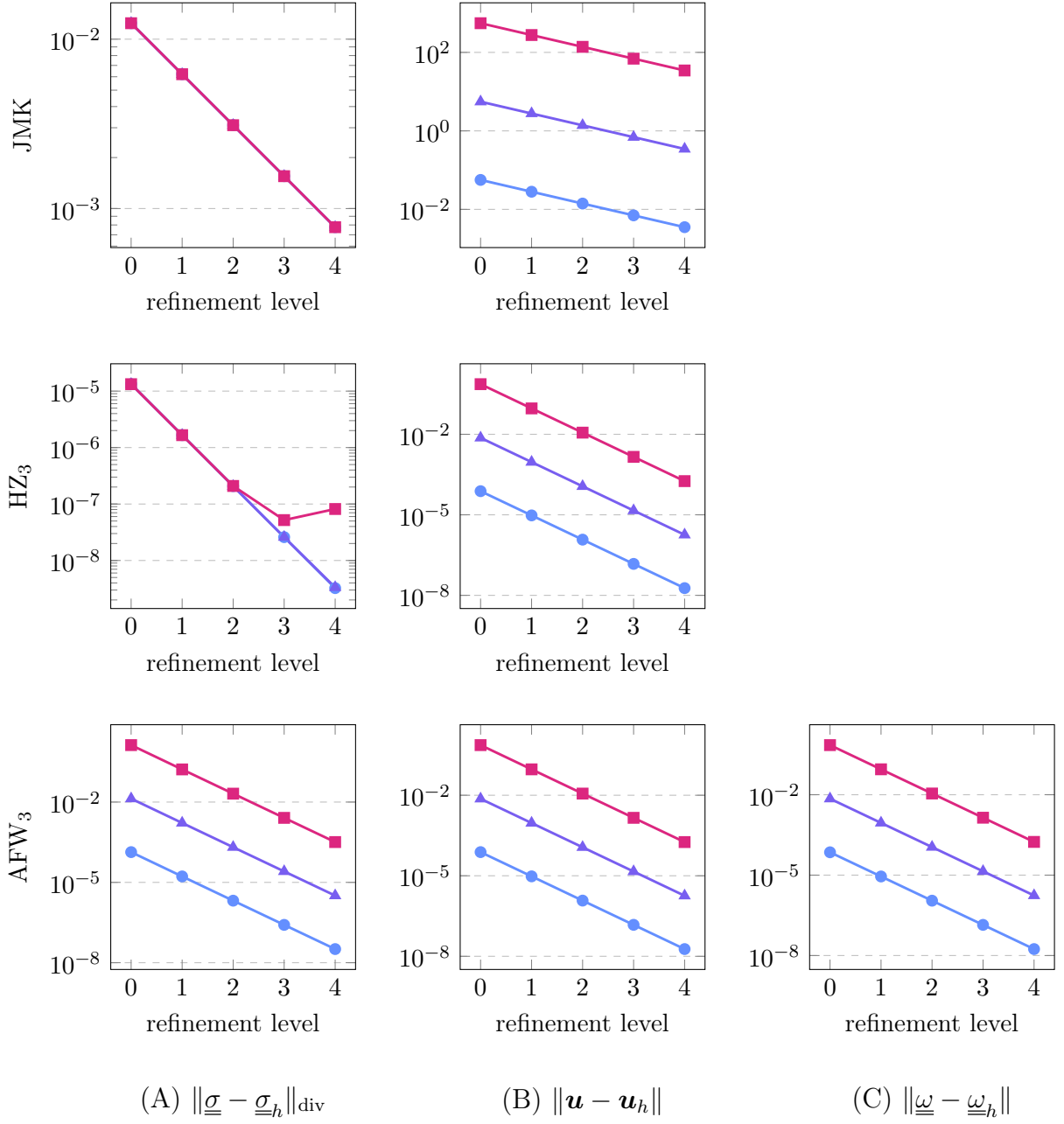


Figure 6: Numerical results for the 2D polar fluid example with a stressed configuration as presented in section 3.4 for  $\delta = 10$  (—●—),  $\delta = 10^3$  (—▲—), and  $\delta = 10^5$  (—■—) with the JMK scheme, the HZ<sub>3</sub> scheme, and the AFW<sub>3</sub> scheme. The errors are displayed as in Figure 1. Observe that the strongly symmetric schemes JMK and HZ<sub>3</sub> produce errors that are independent of  $\delta$ , while the stress errors for AFW<sub>3</sub> are well above solver tolerances and scale like  $\delta$ .

continuously on  $F$  and  $G$ . For instance, we assume that the following inf-sup condition holds:

$$\beta := \inf_{q \in \mathcal{Q}} \sup_{v \in \mathcal{V}} \frac{B(v, q)}{\|v\|_{\mathcal{V}} \|q\|_{\mathcal{Q}}} > 0. \quad (4.2)$$

The particular examples we have seen in section 2 are

- Problem (2.12):  $\mathcal{V} = \Sigma^{\text{sym}}$  and  $\mathcal{Q} = V$  defined in (2.13),  $A(\underline{\sigma}, \underline{\tau}) = a(\underline{\sigma}, \underline{\tau})$  defined in (2.14a), and  $B(\underline{\tau}, \mathbf{v}) = b(\underline{\tau}, \mathbf{v})$  defined in (2.14b).
- Problem (2.18):  $\mathcal{V} = \Sigma$  and  $\mathcal{Q} = V \times \Xi$  defined in (2.13) and (2.19),  $A(\underline{\sigma}, \underline{\tau}) = a(\underline{\sigma}, \underline{\tau})$  defined in (2.14a), and  $B(\underline{\tau}, (\mathbf{v}, \underline{\xi})) = b(\underline{\tau}, \mathbf{v}) + c(\underline{\tau}, \underline{\xi})$  defined in (2.14b) and (2.19).

Let  $\mathcal{V}_h \subset \mathcal{V}$  and  $\mathcal{Q}_h \subset \mathcal{Q}$  denote finite dimensional subspaces and consider the following conforming discretization of (4.1): Find  $u_h \in \mathcal{V}_h$  and  $q_h \in \mathcal{Q}_h$  such that

$$A(u_h, v_h) + B(v_h, p_h) = F(v_h) \quad \forall v_h \in \mathcal{V}_h, \quad (4.3a)$$

$$B(u_h, q_h) = G(q_h) \quad \forall q_h \in \mathcal{Q}_h. \quad (4.3b)$$

Analogous to above, we assume that the discrete Babuška-Brezzi conditions hold (see e.g. [42, Theorem 4.2.3]) so that solutions to (4.3) exist, are unique, and depend continuously on  $F$  and  $G$ . For instance, we assume that the following discrete inf-sup condition holds

$$\beta_h := \inf_{q_h \in \mathcal{Q}_h} \sup_{v_h \in \mathcal{V}_h} \frac{B(v_h, q_h)}{\|v_h\|_{\mathcal{V}} \|q_h\|_{\mathcal{Q}}} > 0. \quad (4.4)$$

#### 4.1. Structure-preservation

The key property of the system (4.1) fundamental to material robustness is the following ‘‘invariance’’ property: If  $F(\cdot)$  is shifted by  $B(\cdot, r)$  for some  $r \in \mathcal{Q}$ , then only the Lagrange multiplier  $p$  is shifted by  $r$ . More precisely, we have the following result.

**Lemma 4.1.** *Let  $F \in \mathcal{V}'$  and  $G \in \mathcal{Q}'$  be given, and let  $u \in \mathcal{V}$  and  $p \in \mathcal{Q}$  satisfy (4.1). Given  $r \in \mathcal{Q}$ , let  $u_r \in \mathcal{V}$  and  $p_r \in \mathcal{Q}$  satisfy*

$$A(u_r, v) + B(v, p_r) = F(v) + B(v, r) \quad \forall v \in \mathcal{V}, \quad (4.5a)$$

$$B(u_r, q) = G(q) \quad \forall q \in \mathcal{Q}. \quad (4.5b)$$

*Then,  $u_r = u$  and  $p_r = p + r$  for all  $r \in \mathcal{Q}$ .*

*Proof.* Direct verification shows that the  $u$  and  $p + r$  satisfy (4.5), and so the result follows by the uniqueness of solutions.  $\square$

In view of Lemma 4.1, we can define one notion of a structure-preserving discretization as follows. For  $r \in \mathcal{Q}$ , let  $u_{h,r} \in \mathcal{V}_h$  and  $p_{h,r} \in \mathcal{Q}_h$  satisfy

$$A(u_{h,r}, v) + B(v, p_{h,r}) = F(v) + B(v, r) \quad \forall v \in \mathcal{V}_h, \quad (4.6a)$$

$$B(u_{h,r}, q) = G(q) \quad \forall q \in \mathcal{Q}_h. \quad (4.6b)$$

Then, we say the discretization  $\mathcal{V}_h \times \mathcal{Q}_h$  of (4.1) is *structure-preserving* if for any choice of  $F \in \mathcal{V}'$  and  $G \in \mathcal{Q}'$ , there holds

$$u_{h,r} = u_h \quad \forall r \in \mathcal{Q}. \quad (4.7)$$

That is, the discrete scheme (4.3) possesses the same invariance property as the continuous problem (4.1). Note that  $u_{h,r} = u_h$  for all  $r \in \mathcal{Q}_h$  by the same reasoning as in Lemma 4.1, and so posing condition (4.7) over all  $r \in \mathcal{Q}$  is nontrivial. In [32, eq. (1.4)] in the context of incompressible flow, property (4.7) is called the ‘‘fundamental invariance property’’.

Another common notion of a structure-preserving scheme arises in the case that  $G \equiv 0$ . Then, the exact solution satisfies

$$u \in \ker \mathcal{B} := \{v \in \mathcal{V} : B(v, q) = 0 \ \forall q \in \mathcal{Q}\}, \quad (4.8)$$

while the discrete solution satisfies

$$u_h \in \ker \mathcal{B}_h := \{v_h \in \mathcal{V}_h : B(v_h, q_h) = 0 \ \forall q_h \in \mathcal{Q}_h\}. \quad (4.9)$$

Here, one may call a scheme structure-preserving if  $\ker \mathcal{B}_h \subseteq \ker \mathcal{B}$ . For example, in incompressible flow problems, the condition  $\ker \mathcal{B}_h \subseteq \ker \mathcal{B}$  means that the discrete flow is pointwise divergence-free (and hence incompressible). The following result shows that these apparently different notions of a structure-preserving scheme actually coincide.

**Lemma 4.2.** *For  $F \in \mathcal{V}'$ ,  $G \in \mathcal{Q}'$ , and  $r \in \mathcal{Q}$ , let  $u_h \in \mathcal{V}_h$  and  $p_h \in \mathcal{Q}_h$  satisfy (4.3) and  $u_{h,r} \in \mathcal{V}_h$  and  $p_{h,r} \in \mathcal{Q}_h$  satisfy (4.6). Then,*

$$u_{h,r} = u_h \quad \forall r \in \mathcal{Q} \iff \ker \mathcal{B}_h \subseteq \ker \mathcal{B}. \quad (4.10)$$

*Proof.* First note that the following holds by definition:

$$B(v_h, r) = 0 \quad \forall v_h \in \ker \mathcal{B}_h, \ \forall r \in \mathcal{Q} \iff \ker \mathcal{B}_h \subseteq \ker \mathcal{B}. \quad (4.11)$$

The differences  $e_{h,r} := u_h - u_{h,r}$  and  $\epsilon_{h,r} := p_h - p_{h,r}$  satisfy

$$\begin{aligned} A(e_{h,r}, v_h) + B(v_h, \epsilon_{h,r}) &= -B(v_h, r) & \forall v_h \in \mathcal{V}_h, \\ B(e_{h,r}, q_h) &= 0 & \forall q_h \in \mathcal{Q}_h. \end{aligned}$$

Taking  $v_h \in \ker \mathcal{B}_h$  then gives

$$A(e_{h,r}, v_h) = -B(v_h, r) \quad \forall v_h \in \ker \mathcal{B}_h.$$

By the well-posedness of (4.3), the above problem is well-posed (see e.g. [42, Theorem 4.2.2]), and so  $e_{h,r} \equiv 0$  if and only if  $B(v_h, r) = 0$  for all  $v_h \in \ker \mathcal{B}_h$ . Thanks to (4.11),  $e_{h,r} \equiv 0$  for all  $r \in \mathcal{Q}$  if and only if  $\ker \mathcal{B}_h \subseteq \ker \mathcal{B}$ .  $\square$

As in Lemma 4.1, we can also obtain an expression for the discrete pressure as follows.

**Lemma 4.3.** *Let  $p_h$  and  $p_{h,r}$  be as in Lemma 4.2 and suppose that  $\ker \mathcal{B}_h \subseteq \ker \mathcal{B}$ . Then, there exists a unique linear projection operator  $\Phi_h : \mathcal{Q} \rightarrow \mathcal{Q}_h$  such that*

$$B(v_h, q - \Phi_h q) = 0 \quad \forall v_h \in \mathcal{V}_h, \forall q \in \mathcal{Q}, \quad (4.12)$$

and  $p_{h,r} = p_h + \Phi_h r$ .

*Proof.* The existence of  $\Phi_h$  is an immediate consequence of [42, Proposition 5.1.2]. For uniqueness, let  $\Psi_h : \mathcal{Q} \rightarrow \mathcal{Q}_h$  be another linear operator satisfying (4.12). Then, for any  $q \in \mathcal{Q}$ , we have

$$B(v_h, (\Phi_h - \Psi_h)q) = 0 \quad \forall v_h \in \mathcal{V}_h.$$

Thanks to the discrete inf-sup condition (4.4), there holds

$$\beta_h \|(\Phi_h - \Psi_h)q\|_{\mathcal{Q}} \leq \sup_{v_h \in \mathcal{V}_h} \frac{B(v_h, (\Phi_h - \Psi_h)q)}{\|v_h\|_{\mathcal{V}_h}} = 0,$$

and so  $\Phi_h q = \Psi_h q$  for all  $q \in \mathcal{Q}$ .

From the proof of Lemma 4.2, we have

$$B(v_h, p_h - p_{h,r}) = -B(v_h, r) = -B(v_h, \Phi_h r) \quad \forall v \in \mathcal{V}_h,$$

where we used (4.12). Arguing as above, we obtain  $p_{h,r} = p_h + \Phi_h r$ . □

**Remark 4.1.** *For some problems, including those in section 3,  $B(\cdot, \cdot)$  is of the form*

$$B(v, q) := (Dv, q)_{\mathcal{Q}},$$

where  $D : \mathcal{V} \rightarrow \mathcal{Q}$  is a bounded linear operator. In this setting,  $\Phi_h$  satisfies

$$(Dv_h, q - \Phi_h q)_{\mathcal{Q}} = 0 \quad \forall v_h \in \mathcal{V}_h, \forall q \in \mathcal{Q}.$$

Thus,  $\Phi_h$  is the  $(\cdot, \cdot)_{\mathcal{Q}}$ -orthogonal projection onto  $D\mathcal{V}_h$ . A common way to ensure that  $\ker \mathcal{B}_h \subseteq \ker \mathcal{B}$  is to choose  $\mathcal{Q}_h = D\mathcal{V}_h$ , in which case  $\Phi_h$  is the  $(\cdot, \cdot)_{\mathcal{Q}}$ -orthogonal projection onto  $\mathcal{Q}_h$ .

#### 4.2. Expressing the examples in the form (4.5)

All the examples in section 3 were constructed to be precisely of the form (4.5) with  $F(\cdot) \equiv 0$ . First consider the strongly symmetric problem (2.12). We choose  $r = \mathbf{w}$  for some  $\mathbf{w} \in \mathcal{Q} = V$ . We cannot choose any  $\mathbf{w}$ , as the constitutive law (2.12a) requires that the RHS has a specific form. In particular, we require that

$$(\nabla \cdot \underline{\boldsymbol{\tau}}, \mathbf{w}) = \langle \underline{\boldsymbol{\tau}} \mathbf{n}, \mathbf{g} \rangle_{\partial\Omega} + (\underline{\boldsymbol{F}}, \underline{\boldsymbol{\tau}}) \quad \forall \underline{\boldsymbol{\tau}} \in \Sigma^{\text{sym}}$$

for some suitable  $\mathbf{g}$  and  $\underline{\underline{F}}$ . Supposing that  $\mathbf{w}$  is smooth enough, we integrate the LHS by parts to obtain

$$\langle \underline{\underline{\tau}}\mathbf{n}, \mathbf{w} \rangle_{\partial\Omega} - (\underline{\underline{\varepsilon}}(\mathbf{w}), \underline{\underline{\tau}}) = \langle \underline{\underline{\tau}}\mathbf{n}, \mathbf{g} \rangle_{\partial\Omega} + (\underline{\underline{F}}, \underline{\underline{\tau}}) \quad \forall \underline{\underline{\tau}} \in \Sigma^{\text{sym}},$$

and so  $\mathbf{g} = \mathbf{w}|_{\partial\Omega}$  and  $\underline{\underline{\varepsilon}}(\mathbf{w}) = -\underline{\underline{F}}$ . Since all domains in section 3 are contractible, such a choice of  $\mathbf{w}$  is possible only if Saint-Venant's compatibility condition holds (see e.g. [52, Theorem 3.2]):  $\nabla^\top \times (\nabla \times \underline{\underline{F}}) = \underline{\underline{0}}$ , where the first curl is taken row-wise and the  $\nabla^\top \times$  denotes the columnwise curl. Provided that  $\underline{\underline{F}}$  satisfies this condition, the equation  $\underline{\underline{\varepsilon}}(\mathbf{w}) = -\underline{\underline{F}}$  can be integrated to find  $\mathbf{w}$ . Of course, this is equivalent to saying that  $\mathbf{w}$  gives rise to a no-stress configuration; i.e.  $\underline{\underline{\sigma}} \equiv \underline{\underline{0}}$  and  $\mathbf{u} = \mathbf{w}$  satisfy (2.9a).

- For linear isotropic materials in section 3.1,  $\underline{\underline{F}} \equiv \underline{\underline{0}}$ , and so the only choices for  $\mathbf{w}$  are rigid body motions, for which (3.1) is one option.
- For the transversely isotropic solid in section 3.2,  $\underline{\underline{F}} = \delta\boldsymbol{\nu} \otimes \boldsymbol{\nu}$ , and so we choose  $\boldsymbol{\nu}$  to satisfy the Saint-Venant's compatibility condition.
- For the polar fluids in sections 3.3 and 3.4, we have  $\underline{\underline{F}} = (K_F \nabla \boldsymbol{\nu}^\top \nabla \boldsymbol{\nu})^D / (2\mu) - (g_{\text{div}}/d)\underline{\underline{\mathbb{I}}}$ . In section 3.3.1, we first choose  $\boldsymbol{\nu} = [x, y]^\top$  so that  $(\nabla \boldsymbol{\nu})^\top \nabla \boldsymbol{\nu} = \underline{\underline{\mathbb{I}}}$  and then find  $\mathbf{w}$  such that  $\underline{\underline{\varepsilon}}(\mathbf{w}) = h(x, y)\underline{\underline{\mathbb{I}}}$ . Then,  $K_F = h(x, y)$  and  $g_{\text{div}} = \nabla \cdot \mathbf{w}$ . In section 3.3.2, we find  $\boldsymbol{\nu}$  such that  $(\nabla \boldsymbol{\nu})^\top \nabla \boldsymbol{\nu}$  satisfies Saint-Venant's compatibility condition.

Thus, the RHS of (2.12a) for all the examples in section 3 is of the form  $b(\underline{\underline{\tau}}, \mathbf{w})$  for suitably chosen  $\mathbf{w}$ .

For the weakly symmetric problem (2.18), we have  $r = (\mathbf{w}, \underline{\underline{\eta}}) \in \mathcal{Q} = V \times \Xi$ . As above, the choice of  $\mathbf{w}$  and  $\underline{\underline{\eta}}$  must match the constitutive law (2.18a):

$$(\nabla \cdot \underline{\underline{\tau}}, \mathbf{w}) + (\underline{\underline{\tau}}, \underline{\underline{\eta}}) = \langle \underline{\underline{\tau}}\mathbf{n}, \mathbf{g} \rangle_{\partial\Omega} + (\underline{\underline{F}}, \underline{\underline{\tau}}) \quad \forall \underline{\underline{\tau}} \in \Sigma.$$

Assuming  $\mathbf{w}$  is sufficiently smooth and integrating by parts gives

$$\langle \underline{\underline{\tau}}\mathbf{n}, \mathbf{w} \rangle_{\partial\Omega} - (\underline{\underline{\tau}}, \nabla \mathbf{w}) + (\underline{\underline{\tau}}, \underline{\underline{\eta}}) = \langle \underline{\underline{\tau}}\mathbf{n}, \mathbf{g} \rangle_{\partial\Omega} + (\underline{\underline{F}}, \underline{\underline{\tau}}) \quad \forall \underline{\underline{\tau}} \in \Sigma,$$

Thus, we must have that  $\mathbf{g} = \mathbf{w}$  and  $-\nabla \mathbf{w} + \underline{\underline{\eta}} = \underline{\underline{F}}$ . Since  $\underline{\underline{F}}$  is symmetric, we have  $\underline{\underline{\varepsilon}}(\mathbf{w}) = -\underline{\underline{F}}$  and  $\underline{\underline{\eta}} = \text{skw}(\nabla \mathbf{w})$ . Thus,  $\mathbf{w}$  is precisely as above with  $\underline{\underline{\eta}} = \text{skw}(\nabla \mathbf{w})$ , and so the RHS of (2.18a) for all the examples in section 3 is of the form  $b(\underline{\underline{\tau}}, \mathbf{w}) + c(\underline{\underline{\tau}}, \underline{\underline{\eta}})$  for suitably chosen  $\mathbf{w}$  and  $\underline{\underline{\eta}}$ .

#### 4.3. Material robustness in the examples

Since all the numerical examples are of the form (4.6), we compare the numerical results from section 3 to Lemma 4.2. For the strongly symmetric discrete formulation (2.15), the JMK and HZ<sub>3</sub> schemes satisfy  $\nabla \cdot \Sigma_h^{\text{sym}} = V_h$ , and so

$$\ker \mathcal{B}_h = \{ \underline{\underline{\tau}}_h \in \Sigma_h^{\text{sym}} : (\nabla \cdot \underline{\underline{\tau}}_h, \mathbf{v}_h)_{L^2(\Omega)} = 0 \forall \mathbf{v}_h \in V_h \} \subset \ker \mathcal{B} = \{ \underline{\underline{\tau}} \in \Sigma^{\text{sym}} : \nabla \cdot \underline{\underline{\tau}} \equiv \mathbf{0} \}.$$

Lemma 4.2 then shows that  $\underline{\underline{\sigma}}_h \equiv \mathbf{0}$  in exact arithmetic for all the examples in sections 3.1 to 3.3 with the JMK or HZ<sub>3</sub> schemes. Thus, any scheme of the form (2.15) with  $\nabla \cdot \Sigma_h^{\text{sym}} = V_h$  is material robust and the numerical results are consistent with the theory (up to roundoff errors and solver tolerances).

For the weakly symmetric discrete formulation (2.15), the situation is more complicated. Now, the discrete kernel  $\ker \mathcal{B}_h$  has the form

$$\ker \mathcal{B}_h = \{ \underline{\underline{\tau}}_h \in \Sigma_h^{\text{sym}} : (\nabla \cdot \underline{\underline{\tau}}_h, \mathbf{v}_h)_{L^2(\Omega)} + (\underline{\underline{\tau}}_h, \underline{\underline{\xi}}_h)_{L^2(\Omega)} = 0 \ \forall \mathbf{v}_h \in V_h, \ \forall \underline{\underline{\xi}}_h \in \Xi_h \}.$$

For all the schemes used in section 3, we still have  $\nabla \cdot \Sigma_h^{\text{sym}} = V_h$  which gives

$$\ker \mathcal{B}_h = \{ \underline{\underline{\tau}}_h \in \Sigma_h^{\text{sym}} : \nabla \cdot \underline{\underline{\tau}}_h \equiv \mathbf{0} \text{ and } (\underline{\underline{\tau}}_h, \underline{\underline{\xi}}_h)_{L^2(\Omega)} = 0 \ \forall \underline{\underline{\xi}}_h \in \Xi_h \}.$$

However, none of the above schemes satisfy  $\text{skw}(\Sigma_h) \subseteq \Xi_h$ , and so  $\ker \mathcal{B}_h \not\subseteq \ker \mathcal{B}$ . That is, there are discrete tensors  $\underline{\underline{\tau}}_h \in \ker \mathcal{B}_h$  that are not pointwise symmetric. Consequently, Lemma 4.1 does not apply and we cannot expect  $\underline{\underline{\sigma}}_h$  to be zero. In the transversely isotropic example in section 3.2, PEERS and AFW<sub>k</sub>,  $k \leq 2$ , both produced nonzero  $\underline{\underline{\sigma}}_h$ . For the polar fluid example in section 3.3, all the weakly symmetric schemes produced nonzero  $\underline{\underline{\sigma}}_h$ , and so the weakly symmetric schemes considered in section 2.3 are not material robust.

In summary, we have the following result:

**Theorem 4.1.** *If a strongly symmetric discretization (2.15) satisfies*

$$\{ \underline{\underline{\tau}}_h \in \Sigma_h^{\text{sym}} : (\nabla \cdot \underline{\underline{\tau}}_h, \mathbf{v}_h)_{L^2(\Omega)} = 0 \ \forall \mathbf{v}_h \in V_h \} \subset \{ \underline{\underline{\tau}} \in \Sigma^{\text{sym}} : \nabla \cdot \underline{\underline{\tau}} \equiv \mathbf{0} \}, \quad (4.13)$$

*then it is material robust. Similarly, if a weakly symmetric discretization (2.20) satisfies*

$$\begin{aligned} \{ \underline{\underline{\tau}}_h \in \Sigma_h : (\nabla \cdot \underline{\underline{\tau}}_h, \mathbf{v}_h)_{L^2(\Omega)} + (\underline{\underline{\tau}}_h, \underline{\underline{\xi}}_h)_{L^2(\Omega)} = 0 \ \forall \mathbf{v}_h \in V_h, \ \forall \underline{\underline{\xi}}_h \in \Xi_h \} \\ \subset \{ \underline{\underline{\tau}} \in \Sigma^{\text{sym}} : \nabla \cdot \underline{\underline{\tau}} \equiv \mathbf{0} \}, \end{aligned} \quad (4.14)$$

*then it is material robust.*

Condition (4.13) may be interpreted as ensuring that in the absence of body forces  $\mathbf{f} = \mathbf{0}$ , the scheme (2.15) produces a stress with zero linear momentum, i.e.  $\text{div } \underline{\underline{\sigma}} = \mathbf{0}$ . Condition (4.14) additionally ensures that the angular momentum is conserved, i.e.  $\underline{\underline{\sigma}}^\top = \underline{\underline{\sigma}}$ .

We have yet to explain the following behavior. For the linear isotropic solid in section 3.1, all the weakly symmetric schemes gave  $\underline{\underline{\sigma}}_h \equiv \underline{\underline{0}}$ , while for the transversely isotropic solid, AFW<sub>3</sub> gave  $\underline{\underline{\sigma}}_h \equiv \underline{\underline{0}}$ . Recall that the key observation was that the rotation tensor  $\underline{\underline{\omega}}$  satisfied  $\underline{\underline{\omega}} \in \Xi_h$  in these cases. To rigorously explain the behavior in this case, we turn a priori error estimates.

#### 4.4. A priori error estimates

As noted in the previous section, Lemma 4.2 is not sufficient to explain the behavior observed in section 3 in all cases, particularly the implication that  $\underline{\underline{\sigma}} \equiv \underline{\underline{0}}$  and  $\underline{\underline{\omega}} \in \Xi_h$

guarantees  $\underline{\sigma}_h \equiv \underline{0}$ . To explain this case, we again return to the abstract setting and establish a priori error estimates, which requires some additional notation. We denote the norms of the bilinear forms  $A(\cdot, \cdot)$  and  $B(\cdot, \cdot)$  by

$$\|A\| := \sup_{\substack{v, w \in \mathcal{V} \\ \|v\|_{\mathcal{V}} = \|w\|_{\mathcal{V}} = 1}} |A(u, v)| \quad \text{and} \quad \|B\| := \sup_{\substack{v \in \mathcal{V}, q \in \mathcal{Q} \\ \|v\|_{\mathcal{V}} = \|q\|_{\mathcal{Q}} = 1}} |B(v, q)|. \quad (4.15)$$

Let  $\mathcal{B} : \mathcal{V} \rightarrow \mathcal{Q}'$  and  $\mathcal{B}^t : \mathcal{Q} \rightarrow \mathcal{V}'$  denote the linear operators associated with the bilinear form  $B(\cdot, \cdot)$ ; i.e.,

$$\mathcal{B}(v)(q) := B(v, q) \quad \text{and} \quad \mathcal{B}^t(q)(v) := B(v, q) \quad \forall v \in \mathcal{V}, \forall q \in \mathcal{Q}.$$

Let  $\mathcal{B}_h : \mathcal{V}_h \rightarrow \mathcal{Q}'_h$  and  $\mathcal{B}_h^t : \mathcal{Q}_h \rightarrow \mathcal{V}'_h$  be defined analogously. Note that the definition of  $\ker \mathcal{B}$  (4.8) and  $\ker \mathcal{B}_h$  (4.9) coincide with the usual notion of the kernel of a linear operator. We similarly use  $\ker \mathcal{B}^t$  and  $\ker \mathcal{B}_h^t$  to denote the corresponding kernels. Given  $F \in \mathcal{V}'$  and  $G \in \mathcal{Q}'$ , we define the following affine spaces:

$$\mathcal{Z}_h^*(F) := \{q_h \in \mathcal{Q}_h : B(v_h, q_h) = F(v_h) \forall v_h \in \mathcal{V}_h\}, \quad (4.16)$$

$$\mathcal{Z}_h(G) := \{v_h \in \mathcal{V}_h : B(v_h, q_h) = G(q_h) \forall q_h \in \mathcal{Q}_h\}. \quad (4.17)$$

Finally, we assume that  $A(\cdot, \cdot)$  is symmetric and satisfies

$$A(v, v) \geq 0 \quad \forall v \in \mathcal{V}, \quad (4.18a)$$

$$A(z, z) \geq \alpha \|z\|_{\mathcal{V}}^2 \quad \forall z \in \ker \mathcal{B}, \quad (4.18b)$$

$$A(z_h, z_h) \geq \alpha_h \|z_h\|_{\mathcal{V}}^2 \quad \forall z_h \in \ker \mathcal{B}_h, \quad (4.18c)$$

for some  $\alpha, \alpha_h > 0$ . Note that all the examples above satisfy (4.18). Strictly speaking, conditions (4.18) can be weakened (see e.g. [42, Theorem 4.2.2]) at the expense of harsher dependence on the constants in all the forthcoming estimates.

Without any additional conditions on  $\mathcal{V}_h$  and  $\mathcal{Q}_h$ , we recall the standard error estimate from [42, Theorem 5.2.2]:

$$\|u - u_h\|_{\mathcal{V}} \leq 2 \left( \frac{\|A\|}{\alpha_h} + \frac{\|B\|}{\beta_h} \sqrt{\frac{\|A\|}{\alpha_h}} \right) \inf_{v_h \in \mathcal{V}_h} \|u - v_h\|_{\mathcal{V}} + \frac{\|b\|}{\alpha_h} \inf_{q_h \in \mathcal{Q}_h} \|p - q_h\|_{\mathcal{Q}} \quad (4.19a)$$

and

$$\begin{aligned} \|p - p_h\|_{\mathcal{Q}} \leq & \left( \frac{2}{\beta_h} \sqrt{\frac{\|A\|^3}{\alpha_h}} + \frac{\|A\| \|B\|}{\beta_h^2} \right) \inf_{v_h \in \mathcal{V}_h} \|u - v_h\|_{\mathcal{V}} \\ & + \frac{3\|B\|}{\beta_h} \sqrt{\frac{\|A\|}{\alpha_h}} \inf_{q_h \in \mathcal{Q}_h} \|p - q_h\|_{\mathcal{Q}}. \end{aligned} \quad (4.19b)$$

We note that these estimates are insufficient to explain the behavior of the numerical examples. In particular, these estimates only guarantee that  $\underline{\sigma}_h \equiv \underline{0}$  for the strongly symmetric schemes if  $\underline{\sigma} \in \Sigma_h$  and  $\mathbf{u} \in V_h$ , while the weakly symmetric schemes additionally require that  $\underline{\omega} \in \Xi_h$ . However, our discrete spaces have additional structure which can be used to obtain better error estimates. We first consider the structure-preserving case  $\ker \mathcal{B}_h \subseteq \ker \mathcal{B}$ , which are satisfied by the strongly symmetric schemes considered here. Then, we will consider the case that  $\mathcal{Q}_h$  is a product of two spaces and the discretizations are only structure-preserving on one of the spaces, as is the case for the weakly symmetric schemes considered here.

#### 4.4.1. Structuring-preserving discretizations

We first assume that the discretization is structure preserving so that  $\ker \mathcal{B}_h \subseteq \ker \mathcal{B}$ . The first error estimate follows from standard arguments (see e.g. [42, Chapter 5.2.2]).

**Lemma 4.4.** *Suppose that  $\ker \mathcal{B}_h \subseteq \ker \mathcal{B}$ . Let  $u \in \mathcal{V}$  and  $p \in \mathcal{Q}$  satisfy (4.1) and  $u_h \in \mathcal{V}_h$  and  $p_h \in \mathcal{Q}_h$  satisfy (4.3). Then, there holds*

$$\|u - u_h\|_{\mathcal{V}} \leq 2\sqrt{\frac{\|A\|}{\alpha_h}} \inf_{w_h \in \mathcal{Z}_h(\mathcal{B}u)} \|u - w_h\|_{\mathcal{V}}, \quad (4.20a)$$

$$\|p - p_h\|_{\mathcal{Q}} \leq \frac{2}{\beta_h} \sqrt{\frac{\|A\|^3}{\alpha_h}} \inf_{w_h \in \mathcal{Z}_h(\mathcal{B}u)} \|u - w_h\|_{\mathcal{V}} + \inf_{r_h \in \mathcal{Z}_h^*(\mathcal{B}^t p)} \|p - r_h\|_{\mathcal{Q}}. \quad (4.20b)$$

*Proof.* Let  $w_h \in \mathcal{Z}_h(G)$ . Then,  $u_h - w_h \in \ker \mathcal{B}_h$ , and there holds

$$A(u_h - w_h, v) = F(v) - A(w_h, v) = A(u - w_h, v) \quad \forall v \in \ker \mathcal{B}_h.$$

Consequently, [42, Lemma 4.3.1] gives

$$\begin{aligned} A(u_h - w_h, u_h - w_h) &= A(u - w_h, u_h - w_h) \\ &\leq \sqrt{A(u - w_h, u - w_h)} \sqrt{A(u_h - w_h, u_h - w_h)}, \end{aligned}$$

and so

$$\alpha_h \|u_h - w_h\|_{\mathcal{V}}^2 \leq A(u_h - w_h, u_h - w_h) \leq A(u - w_h, u - w_h) \leq \|A\| \|u - w_h\|_{\mathcal{V}}^2.$$

Noting that  $\mathcal{Z}_h(G) = \mathcal{Z}_h(\mathcal{B}u)$  and  $\|A\| \geq \alpha_h$ , we apply the triangle inequality to obtain (4.20a). Now, for any  $r_h \in \mathcal{Z}_h^*(\mathcal{B}^t p)$ , we have

$$B(v_h, p_h - r_h) = A(u - u_h, v_h) \quad \forall v_h \in \mathcal{V}_h.$$

The inf-sup condition and (4.20a) then gives

$$\|p_h - r_h\|_{\mathcal{Q}} \leq \frac{2}{\beta_h} \sqrt{\frac{\|A\|^3}{\alpha_h}} \inf_{w_h \in \mathcal{Z}_h(\mathcal{B}u)} \|u - w_h\|_{\mathcal{V}}.$$

Taking the infimum over all such  $r_h$  and applying the triangle inequality completes the proof of (4.20b).  $\square$

Note that the infimums appearing on the RHS of (4.20a) and (4.20b) are restricted to the affine spaces  $\mathcal{Z}_h(\mathcal{B}u)$  and  $\mathcal{Z}_h^*(\mathcal{B}^t p)$ . In some instances, these infimums can be estimated directly to obtain convergence rates (see e.g. [53, Sections 5 & 6] for the infimum in (4.20a) corresponding to the approximation properties of divergence-free, continuous piecewise polynomial vector fields). In other instances, the approximation properties of these affine spaces is less clear.

A classical technique in the literature to obtain an upper bound for the terms in (4.20a) and (4.20b) is to use a Fortin operator (see e.g. [42, Chapter 5.4.3]). Let  $\pi_F : \mathcal{V} \rightarrow \mathcal{V}_h$  be a linear operator satisfying

$$b(v - \pi_F v, q_h) = 0 \quad \forall q_h \in \mathcal{Q}_h, \forall v \in \mathcal{V}, \quad (4.21a)$$

$$\|\pi_F v\|_{\mathcal{V}} \leq C_F \|v\|_{\mathcal{V}} \quad \forall v \in \mathcal{V}, \quad (4.21b)$$

for some  $C_F > 0$ . Since we are assuming that the discrete inf-sup condition (4.4) holds, such an operator always exists with  $C_F \leq \|B\|/\beta_h$  (see e.g. [42, Remark 5.1.10]). However, for some problems, particularly on anisotropic domains,  $C_F$  may be smaller (see [32, Remark 4.1] and references therein). Moreover, let  $C_\Phi$  be the stability constant of the operator  $\Phi_h$  in Lemma 4.3:

$$C_\Phi := \sup_{\substack{q \in \mathcal{Q} \\ \|q\|_{\mathcal{Q}}=1}} \|\Phi_h q\|_{\mathcal{Q}}. \quad (4.22)$$

Note that the inf-sup constant gives  $C_\Phi \leq \|B\|/\beta_h$ , but  $C_\Phi$  may be smaller; e.g.  $C_\Phi = 1$  in the example in Remark 4.1. With these operators in hand, we have the following result.

**Lemma 4.5.** *For all  $u \in \mathcal{V}$ , there holds*

$$\inf_{w_h \in \mathcal{Z}_h(\mathcal{B}u)} \|u - w_h\|_{\mathcal{V}} \leq (1 + C_F) \inf_{v_h \in \mathcal{V}_h} \|u - v_h\|_{\mathcal{V}}. \quad (4.23)$$

Moreover, if  $\ker \mathcal{B}_h \subseteq \ker \mathcal{B}$ , then for all  $p \in \mathcal{Q}$ , there holds

$$\inf_{r_h \in \mathcal{Z}_h^*(\mathcal{B}^t p)} \|p - r_h\|_{\mathcal{Q}} \leq (1 + C_\Phi) \inf_{q_h \in \mathcal{Q}_h} \|p - q_h\|_{\mathcal{Q}}. \quad (4.24)$$

*Proof.* Inequality (4.23) can be found in e.g. [54, Lemma 50.3]. The proof of (4.24) is identical. We include it here for completeness. Let  $q_h \in \mathcal{Q}_h$  and define  $s_h = \Phi_h(p - q_h)$ . Then,  $r_h := s_h + q_h \in \mathcal{Z}_h^*(\mathcal{B}^t p)$  since  $B(v_h, r_h) = B(v_h, p) = (\mathcal{B}^t p)(v_h)$  for all  $v_h \in \mathcal{V}_h$ . Moreover, we have

$$\|p - r_h\|_{\mathcal{Q}} \leq \|p - q_h\|_{\mathcal{Q}} + \|r_h\|_{\mathcal{Q}} \leq (1 + C_\Phi) \|p - q_h\|_{\mathcal{Q}}.$$

The result now follows by first bounding the LHS below by the infimum over all elements in  $\mathcal{Z}_h^*(\mathcal{B}^t p)$  and then taking the infimum over all  $q_h \in \mathcal{Q}_h$ .  $\square$

Combining Lemma 4.4 and Lemma 4.5 gives the following result.

**Corollary 4.1.** *Suppose that  $\ker \mathcal{B}_h \subseteq \ker \mathcal{B}$ . Let  $u \in \mathcal{V}$  and  $p \in \mathcal{Q}$  satisfy (4.1) and  $u_h \in \mathcal{V}_h$  and  $p_h \in \mathcal{Q}_h$  satisfy (4.3). Then, there holds*

$$\|u - u_h\|_{\mathcal{V}} \leq 2(1 + C_F) \sqrt{\frac{\|A\|}{\alpha_h}} \inf_{v_h \in \mathcal{V}_h} \|u - v_h\|_{\mathcal{V}}, \quad (4.25a)$$

$$\|p - p_h\|_{\mathcal{Q}} \leq \frac{2(1 + C_F)}{\beta_h} \sqrt{\frac{\|A\|^3}{\alpha_h}} \inf_{v_h \in \mathcal{V}_h} \|u - v_h\|_{\mathcal{V}} + (1 + C_{\Phi}) \inf_{r_h \in \mathcal{Q}_h} \|p - r_h\|_{\mathcal{Q}}, \quad (4.25b)$$

where  $C_F$  is defined in (4.21b) and  $C_{\Phi}$  in (4.22)

A similar result to Corollary 4.1 appears in [42, Theorem 5.2.4] and [55, Theorem 2] but with harsher dependence on the constants since  $A(\cdot, \cdot)$  is not assumed to be symmetric and nonnegative.

#### 4.4.2. Partially structure-preserving discretizations

We now suppose that  $\mathcal{Q}$  is of the form  $\mathcal{Q} = \mathcal{Q}_1 \times \mathcal{Q}_2$ , where  $\mathcal{Q}_i$  is a Hilbert spaces with inner product  $(\cdot, \cdot)_{\mathcal{Q}_i}$  and induced norm  $\|\cdot\|_{\mathcal{Q}_i}$ ,  $i \in \{1, 2\}$ . We similarly suppose that the discrete space  $\mathcal{Q}_h \subset \mathcal{Q}$  is of the form  $\mathcal{Q}_h = \mathcal{Q}_{1,h} \times \mathcal{Q}_{2,h}$ , where  $\mathcal{Q}_{i,h} \subset \mathcal{Q}_i$ ,  $i \in \{1, 2\}$ .

We consider a bilinear form  $B(\cdot, \cdot)$  and linear functional  $G$  of the form

$$\begin{aligned} B(v, p) &= B_1(v, p_1) + B_2(v, p_2) & \forall p = (p_1, p_2) \in \mathcal{Q}_1 \times \mathcal{Q}_2, \forall v \in \mathcal{V}, \\ G(p) &= G_1(p_1) + G_2(p_2) & \forall p = (p_1, p_2) \in \mathcal{Q}_1 \times \mathcal{Q}_2, \end{aligned}$$

where  $B_i(\cdot, \cdot) : \mathcal{V} \times \mathcal{Q}_i \rightarrow \mathbb{R}$  are continuous bilinear forms with norms  $\|B_i\|$  and  $G_i(\cdot)$  are continuous linear functionals on  $\mathcal{Q}_i$ ,  $i \in \{1, 2\}$ . We define the operators  $\mathcal{B}_i$ ,  $\mathcal{B}_i^t$ ,  $\mathcal{B}_{i,h}$ , and  $\mathcal{B}_{i,h}^t$  and affine spaces  $\mathcal{Z}_{i,h}(G_i)$  and  $\mathcal{Z}_{i,h}^*(F)$  analogously to above.

If we assume that the discretization is only structure-preserving with respect to  $\mathcal{B}_1$  in the sense that  $\ker \mathcal{B}_{1,h} \subseteq \ker \mathcal{B}_1$  but make no additional assumption on  $\ker \mathcal{B}_{2,h}$ , then we have the following error estimates.

**Lemma 4.6.** *Suppose that  $\ker \mathcal{B}_{1,h} \subseteq \ker \mathcal{B}_1$ . Let  $u \in \mathcal{V}$  and  $p = (p_1, p_2) \in \mathcal{Q}_1 \times \mathcal{Q}_2$  satisfy (4.1) and  $u_h \in \mathcal{V}_h$  and  $p_h = (p_{1,h}, p_{2,h}) \in \mathcal{Q}_{1,h} \times \mathcal{Q}_{2,h}$  satisfy (4.3). Then, there holds*

$$\begin{aligned} \|u - u_h\|_{\mathcal{V}} &\leq 2 \left( \frac{\|A\|}{\alpha_h} + \frac{\|B_2\|}{\beta_h} \sqrt{\frac{\|A\|}{\alpha_h}} \right) \inf_{w_h \in \mathcal{Z}_{1,h}(G_1)} \|u - w_h\|_{\mathcal{V}} \\ &\quad + \frac{\|B_2\|}{\alpha_h} \inf_{r_{2,h} \in \mathcal{Q}_{2,h}} \|p_2 - r_{2,h}\|_{\mathcal{Q}_2}, \end{aligned} \quad (4.26a)$$

$$\begin{aligned}
\|p_1 - p_{1,h}\|_{\mathcal{Q}_1} &\leq \left( \frac{2\|A\|^2}{\alpha_h\beta_h} + \frac{4\|B_2\|}{\beta_h^2} \sqrt{\frac{\|A\|^3}{\alpha_h}} + \frac{\|A\|\|B_2\|^2}{\beta_h^3} \right) \inf_{w_h \in \mathcal{Z}_{1,h}(G_1)} \|u - w_h\|_{\mathcal{V}} \\
&\quad + \inf_{r_{1,h} \in \mathcal{Z}_{1,h}^*(\mathcal{B}_1^i p_1)} \|p_1 - r_{1,h}\|_{\mathcal{Q}_1} \\
&\quad + \frac{\|B_2\|}{\beta_h} \left( \frac{\|A\|}{\alpha_h} + \frac{3\|B_2\|}{\beta_h} \sqrt{\frac{\|A\|^3}{\alpha_h}} \right) \inf_{r_{2,h} \in \mathcal{Q}_{2,h}} \|p_2 - r_{2,h}\|_{\mathcal{Q}_2},
\end{aligned} \tag{4.26b}$$

and

$$\begin{aligned}
\|p_2 - p_{2,h}\|_{\mathcal{Q}_2} &\leq \left( \frac{2}{\beta_h} \sqrt{\frac{\|A\|^3}{\alpha_h}} + \frac{\|A\|\|B_2\|}{\beta_h^2} \right) \inf_{w_h \in \mathcal{Z}_{1,h}(G_1)} \|u - w_h\|_{\mathcal{V}} \\
&\quad + \frac{3\|B_2\|}{\beta_h} \sqrt{\frac{\|A\|}{\alpha_h}} \inf_{r_{2,h} \in \mathcal{Q}_{2,h}} \|p_2 - r_{2,h}\|_{\mathcal{Q}_2}.
\end{aligned} \tag{4.26c}$$

*Proof.* Let  $w_h \in \mathcal{Z}_{1,h}(G_1)$  and  $r_{2,h} \in \mathcal{Q}_{2,h}$ . Then, there holds

$$\begin{aligned}
A(u_h - w_h, v_h) + B_2(v_h, p_{2,h} - r_{2,h}) &= A(u - w_h, v_h) + B_2(v_h, p_2 - r_{2,h}), \\
B_2(u_h - w_h, q_{2,h}) &= B_2(u - w_h, q_{2,h}),
\end{aligned}$$

for all  $v_h \in \mathcal{Z}_{1,h}(0)$  and  $q_{2,h} \in \mathcal{Q}_{2,h}$ . First note that the following inf-sup condition restricted to  $\mathcal{Z}_{1,h}(0) \times \mathcal{Q}_{2,h}$  holds for  $B_2$ :

$$\inf_{q_{2,h} \in \mathcal{Q}_{2,h}} \sup_{v_h \in \mathcal{Z}_{1,h}(0)} \frac{B_2(v_h, q_{2,h})}{\|v_h\|_{\mathcal{V}} \|q_{2,h}\|_{\mathcal{Q}_2}} \geq \beta_h. \tag{4.27}$$

Indeed, a consequence full inf-sup condition (4.4) is that for every  $q_{2,h} \in \mathcal{Q}_{2,h}$ , there exists  $v_h \in \mathcal{V}_h$  such that

$$B_1(v_h, r_{1,h}) + B_2(v_h, r_{2,h}) = (q_{2,h}, r_{2,h})_{\mathcal{Q}_2} \quad \forall r_{i,h} \in \mathcal{Q}_{i,h}, i \in \{1, 2\},$$

and  $\|v_h\|_{\mathcal{V}} \leq \beta_h^{-1} \|q_{2,h}\|_{\mathcal{Q}_2}$  (see e.g. [42, Remark 5.1.10]). Clearly,  $v_h \in \mathcal{Z}_{1,h}(0)$ , and so (4.27) follows.

We now apply [42, Theorem 5.2.1] to obtain

$$\begin{aligned}
\|u_h - w_h\|_{\mathcal{V}} &\leq \left( \frac{\|A\|}{\alpha_h} + \frac{2\|B_2\|}{\beta_h} \sqrt{\frac{\|A\|}{\alpha_h}} \right) \|u - w_h\|_{\mathcal{V}} + \frac{\|B_2\|}{\alpha_h} \|p_2 - r_{2,h}\|_{\mathcal{Q}_2} \\
\|p_{2,h} - r_{2,h}\|_{\mathcal{Q}_2} &\leq \left( \frac{2}{\beta_h} \sqrt{\frac{\|A\|^3}{\alpha_h}} + \frac{\|A\|\|B_2\|}{\beta_h^2} \right) \|u - w_h\|_{\mathcal{V}} + \frac{2\|B_2\|}{\beta_h} \sqrt{\frac{\|A\|}{\alpha_h}} \|p_2 - r_{2,h}\|_{\mathcal{Q}_2}.
\end{aligned}$$

Using the triangle inequality and taking the infimum over all  $w_h$  and  $r_{2,h}$  then gives (4.26a) and (4.26c).

We now turn to  $p_1 - p_{1,h}$ . For any  $r_{1,h} \in \mathcal{Z}_{1,h}^*(\mathcal{B}_1^t p_1)$ , there holds

$$B_1(v_h, p_{1,h} - r_{1,h}) = A(u - u_h, v_h) + B_2(v_h, p_2 - p_{2,h}) \quad \forall v_h \in \mathcal{V}_h.$$

Applying the inf-sup condition (4.4), we obtain

$$\|p_{1,h} - r_{1,h}\|_{\mathcal{Q}_1} \leq \frac{\|A\|}{\beta_h} \|u - u_h\|_{\mathcal{V}} + \frac{\|B_2\|}{\beta_h} \|p_2 - p_{2,h}\|_{\mathcal{Q}_2}.$$

Inequality (4.26b) now follows.  $\square$

**Remark 4.2.** *As in Corollary 4.1, we could further replace the infimums in (4.26) by infimums over the full spaces and pick up a factor of  $(1+C_F)$  and  $(1+C_{\Phi_1})$ , where  $\Phi_1 : \mathcal{Q}_1 \rightarrow \mathcal{Q}_{1,h}$  is the operator in Lemma 4.3 for  $B_1$ .*

#### 4.5. Applying error estimates to examples

We now apply the error estimates above to the examples. Note that  $\lambda \in [0, 1] \cup \{\infty\}$ , and so we have  $\|A\| \leq M/\mu$  and  $\alpha_h \geq \alpha/\mu$ , for constants  $M$  and  $\alpha$  independent of  $h$ ,  $\mu$ , and  $\lambda$  (see Lemma A.1 below). Moreover, the ratio  $\|B\|/\beta_h$  is bounded uniformly in  $h$  as we have chosen stable elements. Consequently, we will only highlight the dependence of the constants in the forthcoming error estimates on  $\mu$ .

For the symmetric elements, again assuming that  $\nabla \cdot \Sigma_h^{\text{sym}} = V_h$ , we apply (4.20) to obtain

$$\|\underline{\underline{\sigma}} - \underline{\underline{\sigma}}_h\|_{\text{div}} \leq C \inf_{\underline{\underline{\tau}}_h \in \Sigma_h^{\text{sym}}} \|\underline{\underline{\sigma}} - \underline{\underline{\tau}}_h\|_{\text{div}} \quad (4.28a)$$

$$\|\mathbf{u} - \mathbf{u}_h\| \leq C \left( \frac{1}{\mu} \inf_{\underline{\underline{\tau}}_h \in \Sigma_h^{\text{sym}}} \|\underline{\underline{\sigma}} - \underline{\underline{\tau}}_h\|_{\text{div}} + \inf_{\mathbf{v}_h \in V_h} \|\mathbf{u} - \mathbf{v}_h\| \right). \quad (4.28b)$$

Whenever  $\underline{\underline{\sigma}} \in \Sigma_h^{\text{sym}}$ , we obtain  $\underline{\underline{\sigma}}_h = \underline{\underline{\sigma}}$  from (4.28a), further demonstrating the material robustness property as  $\underline{\underline{0}} \in \Sigma_h^{\text{sym}}$ . More generally, (4.28a) shows that the stress error is independent of the error in  $\mathbf{u}$ , which is consistent with the behavior in section 3.4 where  $\underline{\underline{\sigma}} \neq \underline{\underline{0}}$  but is independent of the scaling parameter  $\delta$ .

For the weakly symmetric elements, also with  $\nabla \cdot \Sigma_h = V_h$ , we apply (4.26) and Remark 4.2 to obtain

$$\|\underline{\underline{\sigma}} - \underline{\underline{\sigma}}_h\|_{\text{div}} \leq C \left( \inf_{\underline{\underline{\tau}}_h \in \Sigma_h} \|\underline{\underline{\sigma}} - \underline{\underline{\tau}}_h\|_{\text{div}} + \mu \inf_{\underline{\underline{\zeta}}_h \in \Xi_h} \|\underline{\underline{\omega}} - \underline{\underline{\zeta}}_h\| \right) \quad (4.29a)$$

$$\|\mathbf{u} - \mathbf{u}_h\| \leq C \left( \frac{1}{\mu} \inf_{\underline{\underline{\tau}}_h \in \Sigma_h} \|\underline{\underline{\sigma}} - \underline{\underline{\tau}}_h\|_{\text{div}} + \inf_{\mathbf{v}_h \in V_h} \|\mathbf{u} - \mathbf{v}_h\| + \inf_{\underline{\underline{\zeta}}_h \in \Xi_h} \|\underline{\underline{\omega}} - \underline{\underline{\zeta}}_h\| \right) \quad (4.29b)$$

$$\|\underline{\underline{\omega}} - \underline{\underline{\omega}}_h\| \leq C \left( \frac{1}{\mu} \inf_{\underline{\underline{\tau}}_h \in \Sigma_h} \|\underline{\underline{\sigma}} - \underline{\underline{\tau}}_h\|_{\text{div}} + \inf_{\underline{\underline{\zeta}}_h \in \Xi_h} \|\underline{\underline{\omega}} - \underline{\underline{\zeta}}_h\| \right). \quad (4.29c)$$

Note that inequality (4.29a) captures the behavior we observed in section 3 — if  $\underline{\sigma} \equiv \underline{0}$  and  $\underline{\omega} \in \Xi_h$ , then  $\underline{\sigma}_h \equiv \underline{0}$ . If  $\underline{\omega} \notin \Xi_h$ , then the error estimates do not guarantee that  $\underline{\sigma}_h \equiv \underline{0}$ , and we indeed observed nonzero  $\underline{\sigma}_h$  in this case, indicating a lack of material robustness.

The construction of the examples in section 3 may also be interpreted as follows. We first find a displacement  $\mathbf{u}^*$  in the kernel of the constitutive law (i.e. (2.8) holds with  $\mathbf{u}^*$  and  $\underline{\sigma}^* = \underline{0}$ ) such that  $\underline{\omega}^* := \text{skw}(\nabla \mathbf{u}^*) \notin \Xi_h$ . We then choose a solution containing a large component of  $\underline{\omega}^*$  (i.e.  $\underline{\omega} = \delta \underline{\omega}^* + \underline{\xi}$  with  $\|\underline{\sigma}\| + \|\underline{\xi}\| \ll \delta \|\underline{\omega}^*\|$ ) to demonstrate that the weakly symmetric schemes produce large errors. This construction is in line with the theory, as the lack of the invariance property (4.7) and the error estimates (4.29) allow the weakly symmetric schemes to produce a much larger stress error (on the order of  $\delta$  as  $\delta \rightarrow \infty$ ) than the strongly symmetric schemes.

#### 4.6. General comments

The error estimates in (4.26) provide a general recipe for demonstrating “non-robustness” of a scheme that is not fully structure-preserving. For example, consider a stable discretization of the saddle-point system (4.1) with  $\|A\| \leq Cv$ ,  $\alpha_h \geq \alpha v$  for some positive parameter  $v$ , and  $\|B\|/\beta_h$  bounded uniformly in  $h$  and  $v$ . Then, (4.26) reads

$$\|u - u_h\|_{\mathcal{V}} \leq C \left( \inf_{w_h \in \mathcal{V}_h} \|u - w_h\|_{\mathcal{V}} + v^{-1} \inf_{r_{2,h} \in \mathcal{Q}_{2,h}} \|p_2 - r_{2,h}\|_{\mathcal{Q}_2} \right) \quad (4.30a)$$

$$\|p_1 - p_{1,h}\|_{\mathcal{Q}_1} \leq C \left( v \inf_{w_h \in \mathcal{V}_h} \|u - w_h\|_{\mathcal{V}} + \inf_{r_{1,h} \in \mathcal{Q}_{1,h}} \|p_1 - r_{1,h}\|_{\mathcal{Q}_1} + \inf_{r_{2,h} \in \mathcal{Q}_{2,h}} \|p_2 - r_{2,h}\|_{\mathcal{Q}_2} \right) \quad (4.30b)$$

$$\|p_2 - p_{2,h}\|_{\mathcal{Q}_2} \leq C \left( v \inf_{w_h \in \mathcal{V}_h} \|u - w_h\|_{\mathcal{V}} + \inf_{r_{2,h} \in \mathcal{Q}_{2,h}} \|p_2 - r_{2,h}\|_{\mathcal{Q}_2} \right), \quad (4.30c)$$

where  $C$  is independent of  $v$  and  $h$ . We will consider  $u_h$  the primary variable of interest. There are two ways to make the error estimate (4.30a) blow up in a meaningful way:

- (i) Fix  $v$  and find a sequence of solutions  $u^k, p_1^k, p_2^k$  such that  $\|u^k\|_{\mathcal{V}}$  is bounded,  $p_2^k \notin \mathcal{Q}_{2,h}$ , and  $\|p_2^k\|_{\mathcal{Q}_2} \rightarrow \infty$  as  $k \rightarrow \infty$ .
- (ii) For a sequence  $v_k \rightarrow 0$ , find solutions  $u^k, p_1^k, p_2^k$  such that  $\|u^k\|_{\mathcal{V}}$  is bounded and  $\inf_{r_{2,h} \in \mathcal{Q}_{2,h}} \|p_2^k - r_{2,h}\|_{\mathcal{Q}_2}$  is bounded away from zero.

In both cases, the best approximation term for  $u_k$  in (4.30a) will remain bounded, while the remaining term in (4.30a) will blow up. In contrast, for either scenario (i) or (ii), the error  $\|u^k - u_h^k\|_{\mathcal{V}}$  for a structure preserving scheme ( $\ker \mathcal{B}_h \subset \ker \mathcal{B}$ ) will not blow up thanks to (4.25) since  $\|u^k\|_{\mathcal{V}}$  is bounded. The examples in section 3 fit into (i). Whether scenario (i) or (ii) can occur for realistic problem settings is application dependent. We note that scenario (i) with  $u^k \equiv 0$ ,  $\mathcal{Q}_1 = \mathcal{Q}_{1,h} = \{0\}$ , and  $v = 1$  is described in [54, Remark 50.8] in the general setting of structure-preserving versus standard discretizations.

In the context of incompressible flow, two commonly used terms are “pressure-robust” [32] and “Reynolds-(semi)-robust” [56] to describe various properties of the discretizations. Pressure robustness typically means that the discrete velocity (and possibly other variables

of interest) are invariant if the external forcing is modified by the gradient of a suitable scalar-valued function. Thus, pressure robustness is precisely the invariance property in (4.7). Recall that Lemma 4.2 shows that the kernel inclusion  $\ker \mathcal{B}_h \subset \ker \mathcal{B}$  is necessary for the discrete scheme to possess this invariance property without modifying the discrete problem. Other methods which modify the functional  $F(\cdot)$  in (4.10) can also achieve the invariance property without requiring  $\ker \mathcal{B}_h \subset \ker \mathcal{B}$ ; see [32, Section 5.2] for a discussion. Reynolds robustness in the context of error estimates typically means that the velocity error (and possibly the errors of other variables) does not blow up (or not blow up too fast) as the viscosity tends to zero. Thus, schemes that are partially structure preserving (see e.g. [9] for a nonconforming scheme) are permitted provided that  $v$  in (4.30) is the inverse of the viscosity.

## 5. Transient Example

We conclude with some comparisons of the JMK and AFW<sub>1</sub> schemes applied to a transient polar fluid. Time-dependent problems are generally outside the framework presented in section 4, as the structure of the variational problem has an additional term (see e.g. (5.2b) below). Nevertheless, we will shortly observe that strongly enforcing symmetry of the Cauchy stress tensor remains crucial for obtaining accurate solutions. We consider the following time-dependent extension of the polar fluid in section 3.3.1 on  $\Omega = (0, 1)^2$ :

$$\partial_t \mathbf{u} - \operatorname{div} \underline{\underline{\sigma}} = 0 \quad \text{in } \Omega \times (0, T), \quad (5.1a)$$

$$\frac{1}{2\mu} \underline{\underline{\sigma}} - \underline{\underline{\varepsilon}}(\mathbf{u}) = \min\{1, t\} \left[ \frac{K_F}{2\mu} (\nabla \boldsymbol{\nu}^\top \nabla \boldsymbol{\nu})^D - \frac{1}{d} (\operatorname{div} \mathbf{u}_0) \mathbb{I} \right] \quad \text{in } \Omega \times (0, T), \quad (5.1b)$$

$$\mathbf{u} = \min\{1, t\} \mathbf{u}_0 \quad \text{on } \partial\Omega \times (0, T), \quad (5.1c)$$

where

$$\boldsymbol{\nu} = \begin{bmatrix} x \\ x + y \end{bmatrix}, \quad K_F(x, y) = \delta \sin(x) \cosh(y), \quad \text{and} \quad \mathbf{u}_0(x, y) = \delta \begin{bmatrix} -\cos(x) \cosh(y) \\ \sin(x) \sinh(y) \end{bmatrix}.$$

We take  $\mu = 1$  and  $\delta = 10^3$ . Note that we have assumed that we are in a regime where the inertial term  $\mathbf{u} \cdot \nabla \mathbf{u}$  is negligible, due to the small velocity and/or high viscosity (after nondimensionalization). The fluid is initially at rest and the boundary conditions and scaling of  $\underline{\underline{F}}$  are chosen to drive the system to an equilibrium state corresponding to the same stress-free state in section 3.3.1.

The corresponding semi-discrete variational formulation with strongly imposed symmetry is: For all  $t \in (0, T)$ , find  $\underline{\underline{\sigma}}_h(t) \in \Sigma_h^{\text{sym}}$  and  $\mathbf{u}_h(t) \in V_h$  such that

$$a(\underline{\underline{\sigma}}_h(t), \underline{\underline{\tau}}_h) + b(\underline{\underline{\tau}}_h, \mathbf{u}_h(t)) = \langle \underline{\underline{\tau}}_h \mathbf{n}, \mathbf{u}_D(t) \rangle_{\partial\Omega} + (\underline{\underline{F}}(t), \underline{\underline{\tau}}_h)_{L^2(\Omega)} \quad \forall \underline{\underline{\tau}}_h \in \Sigma_h^{\text{sym}}, \quad (5.2a)$$

$$b(\underline{\underline{\sigma}}_h(t), \mathbf{v}_h) - (\partial_t \mathbf{u}_h(t), \mathbf{v}_h) = 0 \quad \forall \mathbf{v}_h \in V_h, \quad (5.2b)$$

where  $\underline{\underline{F}}(t)$  is the anisotropic forcing term on the RHS of (5.1b),  $\mathbf{u}_D(t)$  is the boundary condition of the RHS of (5.1c),  $\underline{\underline{\sigma}}_h(0) = \underline{\underline{0}}$ , and  $\mathbf{u}_h(0) = \mathbf{0}$ . Similarly, the semi-discrete

variational formulation with weakly imposed symmetry is: For all  $t \in (0, T)$ , find  $\underline{\sigma}_h(t) \in \Sigma_h$ ,  $\mathbf{u}_h(t) \in V_h$ , and  $\underline{\omega}_h(t) \in \Xi_h$  such that

$$a(\underline{\sigma}_h(t), \underline{\tau}_h) + b(\underline{\tau}_h, \mathbf{u}_h(t)) + c(\underline{\tau}_h, \underline{\omega}_h(t)) = \langle \underline{\tau}_h \mathbf{n}, \mathbf{u}_D(t) \rangle_{\partial\Omega} + (\underline{F}(t), \underline{\tau}_h)_{L^2(\Omega)} \quad \forall \underline{\tau}_h \in \Sigma_h, \quad (5.3a)$$

$$b(\underline{\sigma}_h(t), \mathbf{v}_h) - (\partial_t \mathbf{u}_h(t), \mathbf{v}_h) = 0 \quad \forall \mathbf{v}_h \in V_h, \quad (5.3b)$$

$$c(\underline{\sigma}_h(t), \underline{\xi}_h) = 0 \quad \forall \underline{\xi}_h \in \Xi_h, \quad (5.3c)$$

where  $\underline{\sigma}_h(0) = \underline{0}$ ,  $\mathbf{u}_h(0) = \mathbf{0}$ , and  $\underline{\omega}_h(0) = \underline{0}$ . Since (5.2) and (5.3) are systems of differential-algebraic equations, we discretize in time with a 2-stage Gauss-Radau IIA implicit Runge-Kutta method, automated by the `Irksome` package [57, 58], with a time step size of  $1/100$ . We choose the JMK scheme for (5.2) and the  $\text{AFW}_1$  scheme for (5.3), both on an unstructured mesh of the unit square generated with `ngsPETS` with `maxh = 1/40`. The stage-coupled system is solved via sparse direct LU factorization using `MUMPS` [59].

Snapshots of the magnitudes of the discrete stresses at  $t \in \{0.5, 1, 1.5\}$  are displayed in Figure 7. The discrete stress solutions for  $t > 1.5$ , not shown, are nearly identical to the ones at  $t = 1.5$ . Until  $t = 1$ , both solutions are visually identical. After  $t = 1$ , the material robust scheme JMK relaxes to a zero stress state, the exact steady-state stress, while the scheme  $\text{AFW}_1$  lacking material robustness relaxes to a solution that is far from a zero-stress state. Thus, one should also exercise caution when using schemes that are not material robust for transient problems.

## Appendix A. Well-posedness of (2.12) and (2.18)

We briefly summarize the well-posedness of (2.12) and (2.18). Using the notation of section 4, note that the kernels of the  $\mathcal{B}$  operators of (2.12) and (2.18) take the form

$$\begin{aligned} \{\underline{\tau} \in \Sigma^{\text{sym}} : (\text{div } \underline{\tau}, \mathbf{v})_{L^2(\Omega)} = 0 \ \forall \mathbf{v} \in V\} &= \{\underline{\tau} \in \Sigma^{\text{sym}} : \text{div } \underline{\tau} \equiv \mathbf{0}\}, \\ \{\underline{\tau} \in \Sigma : (\text{div } \underline{\tau}, \mathbf{v})_{L^2(\Omega)} + (\underline{\tau}, \underline{\xi})_{L^2(\Omega)} = 0 \ \forall \mathbf{v} \in V, \ \forall \underline{\xi} \in \Xi\} &= \{\underline{\tau} \in \Sigma^{\text{sym}} : \text{div } \underline{\tau} \equiv \mathbf{0}\}. \end{aligned}$$

The following result shows that the bilinear form  $a(\cdot, \cdot)$  defined in (2.14a) is elliptic on the kernel.

**Lemma A.1.** *For all  $\underline{\tau} \in H(\text{div}; \Omega, \mathbb{R}^{d \times d})$ , there holds*

$$\|\underline{\tau}\|_{L^2(\Omega)} \leq C \left( \|\underline{\tau}^D\|_{L^2(\Omega)} + \|\text{div } \underline{\tau}\|_{L^2(\Omega)} + \left| \int_{\Omega} \text{tr } \underline{\tau} \, dx \right| \right). \quad (\text{A.1})$$

Thus, for all  $\underline{\tau} \in \Sigma$  with  $\text{div } \underline{\tau} \equiv \mathbf{0}$ , there holds

$$\frac{1}{2\mu} \|\underline{\tau}\|_{\text{div}}^2 \leq C_{\lambda} a(\underline{\tau}, \underline{\tau}) \quad \text{where} \quad C_{\lambda} := \begin{cases} C & \text{if } \lambda = \infty, \\ 1 + \frac{d\lambda}{2\mu} & \text{if } \lambda \in [0, \infty). \end{cases}, \quad (\text{A.2})$$

where  $C$  is independent of  $\mu$  and  $\lambda$ .

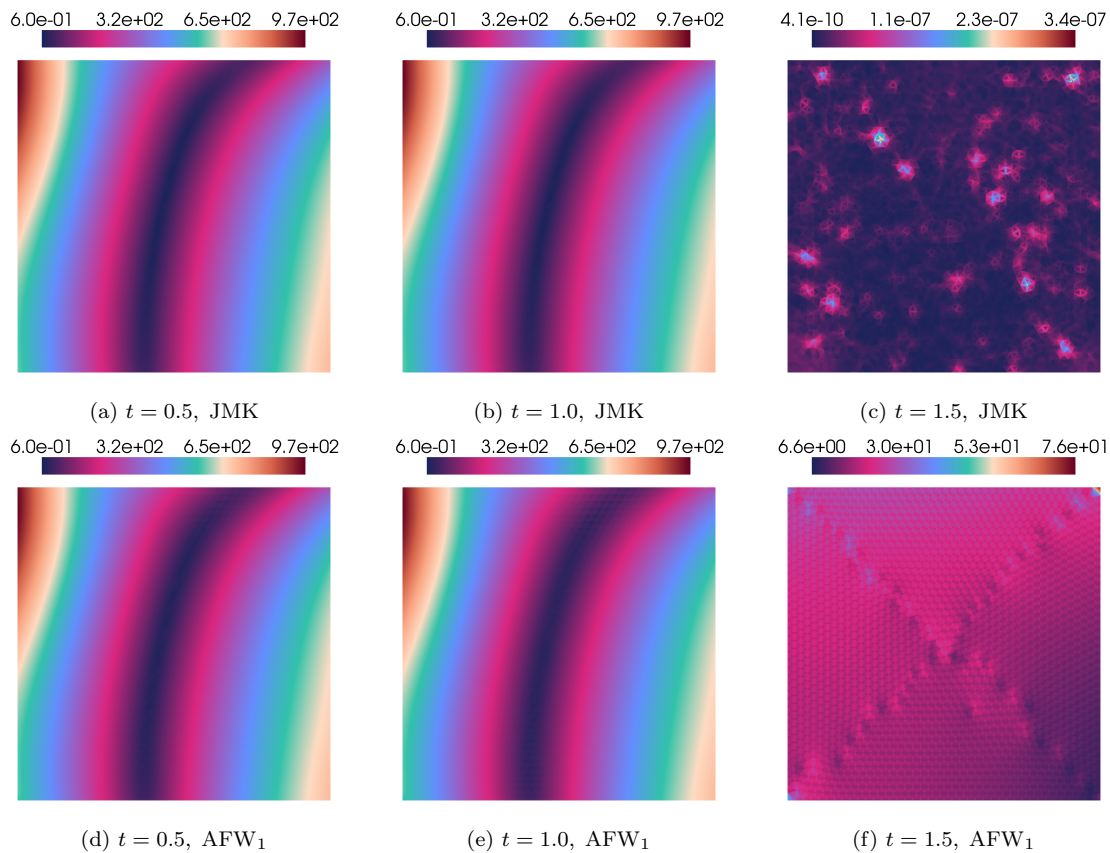


Figure 7: Magnitudes of the stresses for discretizations of a transient 2D polar fluid (5.1). First row: the strongly symmetric scheme JMK (5.2). Second row: the weakly symmetric scheme AFW<sub>1</sub> (5.3). Note that the schemes produce visually identical stress magnitudes until  $t = 1$  (both rows have the same colorbar for these plots). After  $t = 1$ , the strongly symmetric scheme relaxes to a zero stress state, the exact steady state stress, while the weakly symmetric scheme relaxes to a state far from zero. Note that the colorbars for  $t = 1.5$  are different.

*Proof.* Let  $\underline{\underline{\tau}} \in H(\text{div}; \Omega, \mathbb{R}^{d \times d})$ . Thanks to [42, Proposition 9.1.1], there holds

$$\left\| \underline{\underline{\tau}} - \int_{\Omega} \text{tr } \underline{\underline{\tau}} \, dx \right\|_{L^2(\Omega)} \leq C \left( \|\underline{\underline{\tau}}^D\|_{L^2(\Omega)} + \|\text{div } \underline{\underline{\tau}}\|_{L^2(\Omega)} \right),$$

and so (A.1) follows from the triangle inequality. For  $\lambda = \infty$ , inequality (A.2) follows from (A.1) on recalling that if  $\lambda = \infty$  and  $\tau \in \Sigma$ , then  $\int_{\Omega} \text{tr } \tau \, dx = 0$ . For  $\lambda \in [0, \infty)$ , we have

$$\frac{1}{2\mu} \tau : \tau = \frac{1}{2\mu} \tau^D : \tau^D + \frac{1}{2\mu d} (\text{tr } \tau)^2 = \frac{1}{2\mu} \tau^D : \tau^D + \left(1 + \frac{d\lambda}{2\mu}\right) \frac{1}{d(2\mu + d\lambda)} (\text{tr } \tau)^2,$$

and so (A.2) follows on integrating over  $\Omega$ .  $\square$

The remaining ingredients for well-posedness are the inf-sup conditions

$$\beta^{\text{sym}} := \inf_{\mathbf{v} \in V} \sup_{\underline{\underline{\tau}} \in \Sigma^{\text{sym}}} \frac{b(\underline{\underline{\tau}}, \mathbf{v})}{\|\underline{\underline{\tau}}\|_{\text{div}} \|\mathbf{v}\|} > 0 \quad \text{and} \quad \beta := \inf_{\substack{\mathbf{v} \in V \\ \underline{\underline{\xi}} \in \Xi}} \sup_{\underline{\underline{\tau}} \in \Sigma} \frac{b(\underline{\underline{\tau}}, \mathbf{v}) + c(\underline{\underline{\tau}}, \underline{\underline{\xi}})}{\|\underline{\underline{\tau}}\|_{\text{div}} (\|\mathbf{v}\| + \|\underline{\underline{\omega}}\|)} > 0. \quad (\text{A.3})$$

That  $\beta^{\text{sym}} > 0$  follows from the existence of a bounded right inverse of the divergence operator, which we briefly outline here. Let  $\mathbf{v} \in V$  and extend  $\mathbf{v}$  to be zero outside  $\Omega$ . Let  $B \supset \Omega$  be a sufficiently large ball and let  $\mathbf{u} \in \mathbf{H}_0^1(B)$  be the weak solution to following PDE:

$$\text{div } \underline{\underline{\xi}}(\mathbf{u}) = \mathbf{v} \quad \text{in } B \quad \text{and} \quad \mathbf{u}|_{\partial B} = \mathbf{0}.$$

By elliptic regularity (see e.g. [60, p. 263, Lemma 3.2]),  $\mathbf{u} \in \mathbf{H}^2(B)$  with  $\|\mathbf{u}\|_{H^2(B)} \leq C \|\mathbf{v}\|_{L^2(\Omega)}$ , and so  $\text{div } \underline{\underline{\xi}}(\mathbf{u}) = \mathbf{v}$ . Taking  $\underline{\underline{\tau}} = \underline{\underline{\xi}}(\mathbf{u})$  then satisfies  $\text{div } \underline{\underline{\tau}} = \mathbf{v}$  and  $\|\underline{\underline{\tau}}\|_{\text{div}} \leq C \|\mathbf{v}\|$ , and so  $\beta^{\text{sym}} > C^{-1}$ . The proof that  $\beta > 0$  is more involved and can be found in [42, Proposition 9.3.2].

In the literature, the assumption that  $\mathbf{g} \equiv \mathbf{0}$  in (2.9c) is often made for linear elasticity problems where also  $\underline{\underline{F}} \equiv \underline{\underline{0}}$ . In this case, one can test (2.12a) or (2.18a) with  $\underline{\underline{\tau}} = \underline{\underline{I}}$  to see that  $\int_{\Omega} \text{tr } \underline{\underline{\tau}} \, dx = 0$ . Many authors therefore make the choice  $\Sigma^{\text{sym}} = H_*(\text{div}; \Omega, \mathbb{R}_{\text{sym}}^{d \times d})$  and  $\Sigma = \underline{\underline{H}}_*(\text{div}; \Omega, \mathbb{R}^{d \times d})$  so that the coercivity estimate in (A.2) is independent of  $\lambda$ . The resulting schemes are then claimed to be “locking-free,” as the error estimates can be shown to be well-behaved as  $\lambda \rightarrow \infty$ . However, this choice of  $\Sigma^{\text{sym}}$  and  $\Sigma$  only remains valid more generally if one assumes that  $\int_{\partial\Omega} \mathbf{g} \cdot \mathbf{n} \, ds = - \int_{\Omega} \text{tr } \underline{\underline{F}} \, dx$  for  $\lambda < \infty$  (recall that this is precisely the compatibility condition for  $\lambda = \infty$ ). If  $\mathbf{g}$  and  $\underline{\underline{F}}$  do not satisfy this compatibility condition, then one must take  $\Sigma^{\text{sym}}$  and  $\Sigma$  as in (2.13) and (2.19) and the constant  $C_{\lambda}$  in the coercivity estimate (A.2) blows up as  $\lambda \rightarrow \infty$ . Consequently, one obtains error estimates that are not uniform in  $\lambda$ .

## Appendix B. Linear solvers used in section 3

To solve the linear systems arising from (2.15) and (2.20), which are symmetric, we employ MINRES with a standard symmetric block-diagonal preconditioning strategy. For

the strongly symmetric elements (2.15), consider the bilinear form

$$a(\underline{\underline{\sigma}}_h, \underline{\underline{\tau}}_h) + \frac{\mathbb{1}_{\lambda > 10^{10}}}{200d\mu} (\text{tr } \underline{\underline{\sigma}}_h, \text{tr } \underline{\underline{\tau}}_h)_{L^2(\Omega)} + \frac{\gamma}{2\mu} (\text{div } \underline{\underline{\sigma}}_h, \text{div } \underline{\underline{\tau}}_h)_{L^2(\Omega)} + \frac{2\mu}{\gamma} (\mathbf{u}_h, \mathbf{v}_h)_{L^2(\Omega)}, \quad (\text{B.1})$$

where  $\mathbb{1}$  is the indicator function and  $\gamma$  is parameter that we take to be  $10^3$ . Note that for  $\lambda \leq 10^{10}$ , this preconditioner corresponds to a standard augmented Lagrangian preconditioner [61, 62, 63]. The additional term for  $\lambda > 10^{10}$  ensures that form is invertible in floating point arithmetic for  $\lambda \in (10^{10}, \infty]$ . For the weakly symmetric elements (2.20), we add the term  $2\mu(\underline{\underline{\omega}}_h, \underline{\underline{\xi}}_h)_{L^2(\Omega)}$  to (B.1). The resulting preconditioner corresponds to a mix of augmented Lagrangian preconditioning and operator preconditioning [64, 65, 66]. Instead of using (B.1) directly, we apply one multigrid V-cycle with vertex patch preconditioner analogous to [67] for the stress terms and invert the displacement/velocity mass matrix directly. We terminate MINRES when the preconditioned residual decreases by a factor of  $10^{14}$ .

For the case  $\lambda = \infty$ , we do not impose the constraint  $\int_{\Omega} \text{tr } \underline{\underline{\tau}}_h \, dx = 0$  in the implementation. Consequently, the systems (2.15) and (2.20) will have a one dimensional nullspace and  $\underline{\underline{\sigma}}_h$  is unique up to a scalar multiple of  $\underline{\underline{\mathbb{I}}}$ . Nevertheless, the preconditioner (B.1) is invertible, and MINRES still converges. In this case, we also monitor the inexactness condition in [68] with tolerance  $10^{-14}$ . We post-process the final MINRES iterate to satisfy  $\int_{\Omega} \text{tr } \underline{\underline{\sigma}}_h \, dx = \int_{\Omega} \text{tr } \underline{\underline{\sigma}} \, dx$ .

## Appendix C. Pressure-robustness

As mentioned in section 4.6, the structure-preserving property (4.7) is typically called ‘‘pressure robustness’’ in the context of incompressible flow [32]. Here, we show that one obtains similar numerical results as in section 3 for Example 1.1 in [32]. In particular, consider the following Stokes problem on  $\Omega = (0, 1)^2$ : Find  $\mathbf{u} \in H_0^1(\Omega; \mathbb{R}^2)$  and  $p \in L_0^2(\Omega)$  such that

$$(\underline{\underline{\varepsilon}}(\mathbf{u}), \underline{\underline{\varepsilon}}(\mathbf{v}))_{L^2(\Omega)} - (\text{div } \mathbf{v}, p)_{L^2(\Omega)} = (\mathbf{f}, \mathbf{v})_{L^2(\Omega)} \quad \forall \mathbf{v} \in H_0^1(\Omega; \mathbb{R}^2), \quad (\text{C.1a})$$

$$-(\text{div } \mathbf{u}, q)_{L^2(\Omega)} = 0 \quad \forall q \in L_0^2(\Omega), \quad (\text{C.1b})$$

where the forcing term  $\mathbf{f}$  is chosen such that the exact solution is given by

$$\mathbf{f} = \begin{pmatrix} 0 \\ \text{Ra}(1 - y + 3y^2) \end{pmatrix}, \quad \mathbf{u} = \begin{pmatrix} 0 \\ 0 \end{pmatrix}, \quad p = \text{Ra} \left( y^3 - \frac{1}{2}y^2 + y - \frac{7}{12} \right)$$

for a positive parameter  $\text{Ra} > 0$ . Here,  $L_0^2(\Omega)$  denotes mean-free  $L^2(\Omega)$  functions. Note that

$$(\mathbf{f}, \mathbf{v})_{L^2(\Omega)} = -(\text{div } \mathbf{v}, p)_{L^2(\Omega)},$$

which is precisely of the form (4.5) with  $F \equiv 0$  and  $G \equiv 0$ .

We mesh  $\Omega$  as in section 3 with  $\text{maxh} = 1/8$ . We discretize (C.1) with the lowest-order Hood–Taylor (HT) element  $\mathcal{CG}_2(\mathcal{T}_h)^2 \times \mathcal{CG}_1(\mathcal{T}_h)$  and the quadratic Scott–Vogelius (SV) element  $\mathcal{CG}_2(\mathcal{T}_h^{\text{bary}})^2 \times \mathcal{P}_1(\mathcal{T}_h^{\text{bary}})$ , where  $\mathcal{T}_h^{\text{bary}}$  is the barycentric refinement of the mesh. Both

elements are inf-sup stable, but the HT elements are not structure-preserving (pressure-robust), while the SV elements are structure-preserving. We note that numerical results for the HT element also appear in [32], but a structure-preserving method in the sense of (4.7) was not considered for this example in [32]. The direct LU solver MUMPS [59] is used to invert the linear systems. The numerical results for  $Ra \in \{10, 10^3, 10^5\}$  in Figure C.8 are analogous to the results in section 3: The structure-preserving SV elements produce small velocity errors that are on the order of machine precision for  $Ra = 1$  and scale linearly in  $Ra$ , while the HT elements produce nonnegligible velocity errors that also scale with  $Ra$ , but converge to zero quadratically as the mesh is refined. Note that the theory in section 4 applies here as well, and so the SV element produces a zero velocity in exact arithmetic. However, the effect of roundoff errors and scaling the right-hand side of the linear system by  $Ra$  together produce the behavior in Figure C.8.

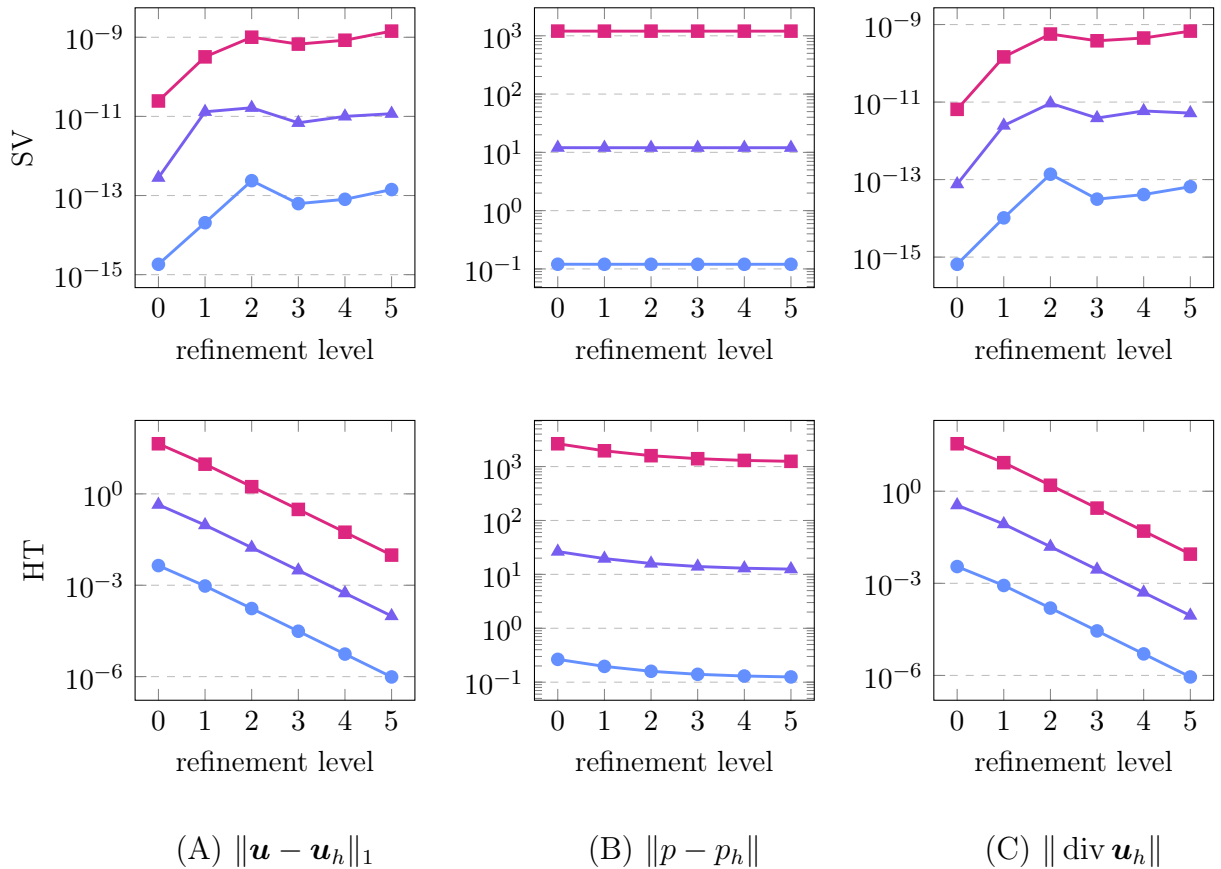


Figure C.8: Numerical results for the Stokes problem (C.1) for  $Ra = 10$  ( $\bullet$ ),  $Ra = 10^3$  ( $\blacktriangle$ ), and  $Ra = 10^5$  ( $\blacksquare$ ) with the SV (first row) and HT (second row) schemes. (A) the velocity errors in  $H^1(\Omega; \mathbb{R}^2)$ , (B) the pressure errors in  $L^2(\Omega)$ , and (C) the divergence errors of the velocity in  $L^2(\Omega)$ . Observe that the non-structure-preserving scheme HT produces significantly larger velocity errors in both (A) and (C) than the structure-preserving SV scheme.

## References

- [1] S. R. Eugster, Hellinger’s 1913 encyclopedia article on the fundamentals of the mechanics of continua, in: F. dell’Isola, S. R. Eugster, M. Spagnuolo, E. Barchiesi (Eds.), *Evaluation of Scientific Sources in Mechanics: Heiberg’s Prolegomena to the Works of Archimedes and Hellinger’s Encyclopedia Article on Continuum Mechanics*, Springer International Publishing, Cham, 2022, pp. 99–313. doi:10.1007/978-3-030-80550-0\_3.
- [2] E. Hellinger, Die allgemeinen ansätze der mechanik der kontinua, in: F. Klein, C. Müller (Eds.), *Encyclopädie der Mathematischen Wissenschaften mit Einschluss ihrer Anwendungen*, volume 4, Leipzig, 1913, pp. 601–694.
- [3] E. Reissner, On a variational theorem in elasticity, *J. Math. Physics* 29 (1950) 90–95. doi:10.1002/sapm195029190.
- [4] E. Reissner, On a variational theorem for finite elastic deformations, *J. Math. Physics* 32 (1953) 129–135. doi:10.1002/sapm1953321129.
- [5] P. G. Ciarlet, L. Gratie, C. Mardare, Intrinsic methods in elasticity: A mathematical survey, *Discrete Contin. Dyn. Syst.* 23 (2009) 133–164. doi:10.3934/dcds.2009.23.133.
- [6] A. Sky, M. Neunteufel, J. S. Hale, A. Zilian, A Reissner-Mindlin plate formulation using symmetric Hu-Zhang elements via polytopal transformations, *Comput. Methods Appl. Mech. Engrg.* 416 (2023) Paper No. 116291, 29. doi:10.1016/j.cma.2023.116291.
- [7] A. Dziubek, K. Hu, M. Karow, M. Neunteufel, Intrinsic mixed finite element methods for linear Cosserat elasticity, *SIAM J. Numer. Anal.* 63 (2025) 1833–1860. doi:10.1137/24M1706578.
- [8] P. Neff, J. Jeong, A new paradigm: The linear isotropic Cosserat model with conformally invariant curvature energy, *ZAMM Z. Angew. Math. Mech.* 89 (2009) 107–122. doi:10.1002/zamm.200800156.
- [9] J. Gopalakrishnan, P. L. Lederer, J. Schöberl, A mass conserving mixed stress formulation for Stokes flow with weakly imposed stress symmetry, *SIAM J. Numer. Anal.* 58 (2020) 706–732. doi:10.1137/19M1248960.
- [10] F. R. A. Aznaran, P. E. Farrell, C. W. Monroe, A. J. Van-Brunt, Finite element methods for multicomponent convection-diffusion, *IMA J. Numer. Anal.* 45 (2025) 188–222. doi:10.1093/imanum/drae001.
- [11] S. Adams, B. Cockburn, A mixed finite element method for elasticity in three dimensions, *J. Sci. Comput.* 25 (2005) 515–521. doi:10.1007/s10915-004-4807-3.
- [12] D. N. Arnold, G. Awanou, R. Winther, Finite elements for symmetric tensors in three dimensions, *Math. Comp.* 77 (2008) 1229–1251. doi:10.1090/S0025-5718-08-02071-1.

- [13] D. N. Arnold, R. Winther, Mixed finite elements for elasticity, *Numer. Math.* 92 (2002) 401–419. doi:10.1007/s002110100348.
- [14] J. Hu, S. Zhang, A family of conforming mixed finite elements for linear elasticity on triangular grids (2015). [arXiv:1406.7457](https://arxiv.org/abs/1406.7457).
- [15] J. Hu, S. Zhang, A family of symmetric mixed finite elements for linear elasticity on tetrahedral grids, *Sci. China Math.* 58 (2015) 297–307. doi:10.1007/s11425-014-4953-5.
- [16] L. Chen, X. Huang, Hybridizable symmetric stress elements on the barycentric refinement in arbitrary dimensions, *Math. Comp.* (electronically published on December 31, 2025, to appear in print). doi:10.1090/mcom/4180.
- [17] S. Gong, J. Gopalakrishnan, J. Guzmán, M. Neilan, Discrete elasticity exact sequences on Worsey-Farin splits, *ESAIM Math. Model. Numer. Anal.* 57 (2023) 3373–3402. doi:10.1051/m2an/2023084.
- [18] J. Gopalakrishnan, J. Guzmán, J. J. Lee, The Johnson-Křížek-mercier elasticity element in higher dimensions, *J. Numer. Math.* (2025). doi:10.1515/jnma-2025-0020.
- [19] C. Johnson, B. Mercier, Some equilibrium finite element methods for two-dimensional elasticity problems, *Numer. Math.* 30 (1978) 103–116. doi:10.1007/BF01403910.
- [20] V. B. Watrood, B. J. Hartz, An equilibrium stress field model for finite element solutions of two-dimensional elastostatic problems, *Int. J. Solids Struct.* 4 (1968) 857–873. doi:10.1016/0020-7683(68)90083-8.
- [21] S. H. Christiansen, J. Gopalakrishnan, J. Guzmán, K. Hu, A discrete elasticity complex on three-dimensional Alfeld splits, *Numer. Math.* 156 (2024) 159–204. doi:10.1007/s00211-023-01381-9.
- [22] M. Amara, J. M. Thomas, Equilibrium finite elements for the linear elastic problem, *Numer. Math.* 33 (1979) 367–383. doi:10.1007/BF01399320.
- [23] D. N. Arnold, F. Brezzi, J. Douglas, Jr., PEERS: A new mixed finite element for plane elasticity, *Japan J. Appl. Math.* 1 (1984) 347–367. doi:10.1007/BF03167064.
- [24] D. N. Arnold, R. S. Falk, R. Winther, Mixed finite element methods for linear elasticity with weakly imposed symmetry, *Math. Comp.* 76 (2007) 1699–1723. doi:10.1090/S0025-5718-07-01998-9.
- [25] D. Boffi, F. Brezzi, M. Fortin, Reduced symmetry elements in linear elasticity, *Commun. Pure Appl. Anal.* 8 (2009) 95–121. doi:10.3934/cpaa.2009.8.95.
- [26] B. Cockburn, J. Gopalakrishnan, J. Guzmán, A new elasticity element made for enforcing weak stress symmetry, *Math. Comp.* 79 (2010) 1331–1349. doi:10.1090/S0025-5718-10-02343-4.

- [27] M. Farhloul, M. Fortin, Dual hybrid methods for the elasticity and the Stokes problems: a unified approach, *Numer. Math.* 76 (1997) 419–440. doi:10.1007/s002110050270.
- [28] J. Gopalakrishnan, J. Guzmán, A second elasticity element using the matrix bubble, *IMA J. Numer. Anal.* 32 (2012) 352–372. doi:10.1093/imanum/drq047.
- [29] R. Stenberg, A family of mixed finite elements for the elasticity problem, *Numer. Math.* 53 (1988) 513–538. doi:10.1007/BF01397550.
- [30] P. L. Lederer, R. Stenberg, Energy norm analysis of exactly symmetric mixed finite elements for linear elasticity, *Math. Comp.* 92 (2023) 583–605. doi:10.1090/mcom/3784.
- [31] P. L. Lederer, R. Stenberg, Analysis of weakly symmetric mixed finite elements for elasticity, *Math. Comp.* 93 (2024) 523–550. doi:10.1090/mcom/3865.
- [32] V. John, A. Linke, C. Merdon, M. Neilan, L. G. Rebholz, On the divergence constraint in mixed finite element methods for incompressible flows, *SIAM Rev.* 59 (2017) 492–544. doi:10.1137/15M1047696.
- [33] J. Schöberl, NETGEN an advancing front 2D/3D-mesh generator based on abstract rules, *Comput. Vis. Sci.* 1 (1997). doi:10.1007/s007910050004.
- [34] J. Schöberl, C++11 Implementation of Finite Elements in NGSolve, Technical Report ASC Report 30/2014, Institute for Analysis and Scientific Computing, Vienna University of Technology, 2014. URL: [https://ngsolve.org/\\_static/ngs-cpp11.pdf](https://ngsolve.org/_static/ngs-cpp11.pdf).
- [35] F. R. A. Aznaran, P. E. Farrell, R. C. Kirby, Transformations for Piola-mapped elements, 2022. doi:10.5802/smai-jcm.91.
- [36] P. D. Brubeck, R. C. Kirby, FIAT: Enabling classical and modern macroelements (2025). arXiv:2501.14599.
- [37] D. A. Ham, P. H. J. Kelly, L. Mitchell, C. J. Cotter, R. C. Kirby, K. Sagiya, N. Bouziani, S. Vorderwuelbecke, T. J. Gregory, J. Betteridge, D. R. Shapero, R. W. Nixon-Hill, C. J. Ward, P. E. Farrell, P. D. Brubeck, I. Marsden, T. H. Gibson, M. Homolya, T. Sun, A. T. T. McRae, F. Luporini, A. Gregory, M. Lange, S. W. Funke, F. Rathgeber, G.-T. Bercea, G. R. Markall, Firedrake User Manual, first edition ed., Imperial College London and University of Oxford and Baylor University and University of Washington, 2023. doi:10.25561/104839.
- [38] M. Křížek, An equilibrium finite element method in three-dimensional elasticity, *Apl. Mat.* 27 (1982) 46–75. URL: <http://eudml.org/doc/15223>, with a loose Russian summary.
- [39] O. Gonzalez, A. M. Stuart, A first course in continuum mechanics, Cambridge Texts in Applied Mathematics, Cambridge University Press, Cambridge, 2008. doi:10.1017/CB09780511619571.

- [40] K. R. Rajagopal, Remarks on the notion of “pressure”, *Int. J. Non-linear Mech.* 71 (2015) 165–172. doi:10.1016/j.ijnonlinmec.2014.11.031.
- [41] Z. Cai, B. Lee, P. Wang, Least-squares methods for incompressible Newtonian fluid flow: linear stationary problems, *SIAM J. Numer. Anal.* 42 (2004) 843–859. doi:10.1137/S0036142903422673.
- [42] D. Boffi, F. Brezzi, M. Fortin, *Mixed finite element methods and applications*, volume 44 of *Springer Series in Computational Mathematics*, Springer, Heidelberg, 2013. doi:10.1007/978-3-642-36519-5.
- [43] P.-A. Raviart, J. M. Thomas, A mixed finite element method for 2nd order elliptic problems, in: *Mathematical aspects of finite element methods (Proc. Conf., Consiglio Naz. delle Ricerche (C.N.R.), Rome, 1975)*, volume Vol. 606 of *Lecture Notes in Math.*, Springer, Berlin-New York, 1977, pp. 292–315. doi:10.1007/BFb0064470.
- [44] F. Brezzi, J. Douglas, Jr., L. D. Marini, Two families of mixed finite elements for second order elliptic problems, *Numer. Math.* 47 (1985) 217–235. doi:10.1007/BF01389710.
- [45] J. Betteridge, P. E. Farrell, M. Hochsteger, C. Lackner, J. Schöberl, S. Zampini, U. Zerbinati, ngsPETSc: A coupling between NETGEN/NGSolve and PETSc, *J. Open Source Softw.* 9 (2024) 7359. doi:10.21105/joss.07359.
- [46] P. D. Brubeck, C. Parker, U. Zerbinati, Software used in ‘Achieving Material Robustness via Symmetric Stress Finite Element Discretizations’, 2026. doi:10.5281/zenodo.20312259.
- [47] J. L. Ericksen, Transversely isotropic fluids, *Colloid and polymer science* 173 (1960) 117–122. doi:10.1007/BF01502416.
- [48] J. Merodio, R. Ogden, Mechanical response of fiber-reinforced incompressible nonlinearly elastic solids, *International Journal of Non-Linear Mechanics* 40 (2005) 213–227. doi:10.1016/j.ijnonlinmec.2004.05.003, special Issue in Honour of C.O. Horgan.
- [49] F. M. Leslie, Theory of flow phenomena in liquid crystals, volume 4 of *Advances in Liquid Crystals*, Elsevier, 1979, pp. 1–81. doi:10.1016/B978-0-12-025004-2.50008-9.
- [50] F. M. Leslie, Continuum theory for nematic liquid crystals, *Continuum Mechanics and Thermodynamics* 4 (1992) 167–175. doi:10.1007/BF01130288.
- [51] P. E. Farrell, G. Russo, U. Zerbinati, Kinetic derivation of an inviscid compressible Leslie–Ericksen equation for rarified calamitic gases, *Multiscale Modeling & Simulation* 22 (2024) 1585–1607. doi:10.1137/24M1630529.
- [52] C. Amrouche, P. G. Ciarlet, L. Gratie, S. Kesavan, On Saint Venant’s compatibility conditions and Poincaré’s lemma, *C. R. Math. Acad. Sci. Paris* 342 (2006) 887–891. doi:10.1016/j.crma.2006.03.026.

- [53] I. Babuška, M. Suri, Locking effects in the finite element approximation of elasticity problems, *Numer. Math.* 62 (1992) 439–463. doi:10.1007/BF01396238.
- [54] A. Ern, J.-L. Guermond, Finite elements II—Galerkin approximation, elliptic and mixed PDEs, volume 73 of *Texts in Applied Mathematics*, Springer, Cham, 2021. doi:10.1007/978-3-030-56923-5.
- [55] R. S. Falk, J. E. Osborn, Error estimates for mixed methods, *RAIRO Anal. Numér.* 14 (1980) 249–277. URL: [https://www.numdam.org/item/M2AN\\_1980\\_\\_14\\_3\\_249\\_0/](https://www.numdam.org/item/M2AN_1980__14_3_249_0/).
- [56] P. W. Schroeder, C. Lehrenfeld, A. Linke, G. Lube, Towards computable flows and robust estimates for inf-sup stable FEM applied to the time-dependent incompressible Navier-Stokes equations, *SeMA J.* 75 (2018) 629–653. doi:10.1007/s40324-018-0157-1.
- [57] P. E. Farrell, R. C. Kirby, J. Marchena-Menéndez, Irksome: automating Runge-Kutta time-stepping for finite element methods, *ACM Trans. Math. Software* 47 (2021) Art. 30, 26. doi:10.1145/3466168.
- [58] R. C. Kirby, S. P. Maclachlan, Extending *irksome*: improvements in automated Runge-Kutta time stepping for finite element methods, *ACM Trans. Math. Software* 51 (2025) Art. 17, 27. doi:10.1145/3759245.
- [59] P. R. Amestoy, I. S. Duff, J.-Y. L’Excellent, J. Koster, A fully asynchronous multifrontal solver using distributed dynamic scheduling, *SIAM J. Matrix Anal. Appl.* 23 (2001) 15–41. doi:10.1137/S0895479899358194.
- [60] J. Nečas, Direct methods in the theory of elliptic equations, Springer Monographs in Mathematics, Springer, Heidelberg, 2012. doi:10.1007/978-3-642-10455-8, translated from the 1967 French original by Gerard Tronel and Alois Kufner, Editorial coordination and preface by Šárka Nečasová and a contribution by Christian G. Simader.
- [61] M. Benzi, M. A. Olshanskii, An augmented Lagrangian-based approach to the Oseen problem, *SIAM J. Sci. Comput.* 28 (2006) 2095–2113. doi:10.1137/050646421.
- [62] R. Hiptmair, T. Schiekofer, B. Wohlmuth, Multilevel preconditioned augmented Lagrangian techniques for 2nd order mixed problems, *Computing* 57 (1996) 25–48. doi:10.1007/BF02238356.
- [63] P. S. Vassilevski, J. P. Wang, Multilevel iterative methods for mixed finite element discretizations of elliptic problems, *Numer. Math.* 63 (1992) 503–520. doi:10.1007/BF01385872.
- [64] R. Hiptmair, Operator preconditioning, *Comput. Math. Appl.* 52 (2006) 699–706. doi:10.1016/j.camwa.2006.10.008.

- [65] R. C. Kirby, From functional analysis to iterative methods, *SIAM Rev.* 52 (2010) 269–293. doi:10.1137/070706914.
- [66] K.-A. Mardal, R. Winther, Preconditioning discretizations of systems of partial differential equations, *Numer. Linear Algebra Appl.* 18 (2011) 1–40. doi:10.1002/nla.716.
- [67] D. N. Arnold, R. S. Falk, R. Winther, Multigrid in  $H(\text{div})$  and  $H(\text{curl})$ , *Numer. Math.* 85 (2000) 197–217. doi:10.1007/PL00005386.
- [68] Y. Liu, F. Roosta, A Newton-MR algorithm with complexity guarantees for nonconvex smooth unconstrained optimization, 2023. arXiv:2208.07095.